Optimization of Sandy Soil Stabilization using a Chemical & Soil Binder Stabilizer

Md. Samnani Sarker, 190051148

Md. Zarif Hossain, 190051150

G M Niher Al Islam Junaid, 190051223

A THESIS SUBMITTED FOR THE DEGREE OF BACHELOR OF SCIENCE IN CIVIL ENGINEERING

Department of Civil and Environmental Engineering

ISLAMIC UNIVERSITY OF TECHNOLOGY (IUT)

2024

APPROVAL

The thesis titled "Optimization of Sandy Soil Stabilization using a Chemical & Soil Binder Stabilizer" submitted by Md. Samnani Sarker, Md. Zarif Hossain and G M Niher Al Islam Junaid, Student No. 190051148, 190051150, and 190051223 has been found as satisfactory and accepted as partial fulfilment of the requirement for the Degree Bachelor of Science in Civil Engineering.

SUPERVISOR

Dr. Hossain Md. Shahin

Professor

Department of Civil and Environment Engineering (CEE)

Islamic University of Technology (IUT)

Board Bazar, Gazipur, Bangladesh

DECLARATION OF CANDIDATES

We hereby certify that we, under the direction of Professor Dr. Hossain Md. Shahin conducted the undergraduate research described in this thesis, and we have not submitted this work elsewhere for any purpose (except for publication).

Dr. Hossain Md. Shahin

Professor,
Department of Civil and Environmental Engineering (CEE)
Islamic University of Technology (IUT)
Board Bazar, Gazipur, Bangladesh

Md. Samnani Sarker
Student No: 190051148
Academic Year: 2023-2024
Date:

Md. Zarif Hossain
Student No: 190051150
Academic Year: 2023-2024
Date:

G M Niher Al Islam Junaid
Student No: 190051223
Academic Year: 2023-2024
Date:

DEDICATION

We dedicate our combined thesis work to our individual parents, families, and friends. We also express our gratitude to Professor Dr. Hossain Md. Shahin, our esteemed supervisor. This is a little gesture of appreciation to everyone who helped us along the way and inspired us to continue going until the very end.

ACKNOWLEDGEMENTS

"In the name of Allah, Most Gracious, Most Merciful"

All the praises to Allah (SWT) who has blessed us with the opportunity to complete this book. Our earnest gratitude towards our supervisor Professor Dr. Hossain Md. Shahin for giving us rightful instructions and for paying attention to us whenever needed throughout the research work. We are greatly indebted to him for enlightening us with his remarks and guidance in order to complete the thesis. We wish to show our gratefulness to 'PRECIOUS ROAD ENGINEERING MANAGEMENT' for providing us the stabilizers. Our expression of gratitude towards all of the departmental faculty members for their aid and support.

We also appreciate all those individuals who have contributed in our work at any scale and those who have showered us with words of encouragement, inspiration and motivation. We are deeply obliged for the collaboration we have received throughout our work.

ABSTRACT

Keywords: *Sandy soil stabilization, Chemical stabilizer, Soil binder, Unconfined Compressive Strength (UCS), California Bearing Ratio (CBR)*

Sandy soils are widespread worldwide and are often discovered in many different regions. The nationwide development of any country takes place rapidly when it has high-rise structures and better transportation facilities, and soil stabilization plays a significant role in supporting these infrastructures. This thesis investigates the application of a chemical stabilizer (TX-95) in combination with a soil binder (SB-95) to optimize the stabilization of sandy soil. The stabilization technique aims to enhance sandy soils, which are frequently characterized by high permeability and poor cohesion, in terms of strength and load-bearing capacity. The impact of the SB-95 content of various compositions was investigated at a constant dosage of the TX-95 throughout different curing periods using a series of laboratory experiments, including the Unconfined Compressive Strength (UCS) test & California Bearing Ratio (CBR) test. The major components of the experiment outcomes demonstrate a substantial improvement in the soil's mechanical properties, increasing the SB-95 content while maintaining a consistent TX-95 dosage. The enhanced soil exhibits phenomenal capabilities in terms of compressive strength and load-bearing capacity, as well as shear strength of up to 825 kPA and CBR value of up to 278%. These findings indicate that the stabilized soil is appropriate for a variety of engineering applications, including bridges, embankments, roads, and the foundation of high-rise structures. The combination of the TX-95 and SB-95 offers an effective stabilization approach for the stabilization of sandy soils, leading significantly to a long-term and sustainable construction practice.

Contents

List of Figures

List of Tables

CHAPTER 1
Introduction

1.1 General

Soil stabilization is a notion that originated back 5000 years ago. People traveled along stable earth roads in ancient Egypt and Mesopotamia. The Greeks and Romans utilized lime to stabilize soils. (Ali Akbar Firoozi1*, 2017) Before the emergence of the Christian Era, it was recognized that some geographic places were impacted by surface materials, making transportation of men and materials problematic due to the ambient conditions along the pathways connecting villages and towns. Mesopotamians and Romans independently discovered how to improve the ability to carry traffic by mixing weak soils with a stabilizing agent such as pulverized limestone or calcium, and this was how the first chemical stabilization of weak soils occurred to improve their load-carrying capacity.

Further research showed that the pavements remained solid and capable of handling growing traffic volume and higher loads in carts and wagons as long as the enhanced soil bases were protected from the adverse consequences of high moisture content through trial and error. The technologically advanced citizens developed stone slabs as wearing surfaces on these conditioned soil substrates. In reality, several Roman-built roads are still in remarkably outstanding condition 2000 years later. (Tim E. Kowalski and Dale W. Starry, 2007)

Soil stabilization is the process that enhances the strength and stability of a soil mass, as well as other engineering and physical characteristics, through various innovations. It is mostly employed when the soil available for construction work is unsuitable for the intended purpose. Stabilization improves engineering performance by improving shear strength of the soil, load-bearing capacity, and shrink-swell properties, reducing the possibility of undesirable engineering behavior such as washing collapse. (Archibong, A REVIEW OF THE PRINCIPLES AND METHODS OF SOIL, 2020)

The stabilization procedure of soil refers to combining two or more distinct types of soils or soil with chemicals that can modify their geotechnical qualities to meet the project's needs. The following are the key characteristics of stabilized soil:

- To increase soil strength, bearing capacity, and other engineering properties
- To control dust at work environments
- To create an indestructible layer to protect natural or manmade structures
- To promote the use of waste materials to stabilize and strengthen soil and sand. (Rahman Izadi, 2022)

Soil stabilization incorporates stabilizing agents (binder materials) into weak soils to enhance geotechnical attributes such as compressibility, strength, permeability, and durability. Stabilization techniques include soils or soil minerals and stabilizing agents or binders. (Makusa, 2012)

Geotechnical engineers classify soil stabilization into two parts:
1. To enhance native soils for the construction of shallow foundations, particularly for roads, airfields, parking lots, and other similar structures.
2. To enhance deep foundation soils or massive soil masses utilized for engineering reasons (e.g., dam and dike construction) by injection treatment, due to their difficulty of access, size, or location. (HANS F. WINTERKORN, 1991)

In road construction projects, the main structure of the road is composed of soil or gravelly material in the pavement layers. The soil used for pavement construction should have precise specifications to ensure the requisite strength against tensile stresses and strains. Unbound materials can be stabilized with cementitious materials using soil stabilization (cement, lime, fly ash, bitumen, or a mixture of these). The stabilized soil components have a higher strength, reduced permeability, and lower compressibility than natural soil. The procedure may be implemented in two ways: 1) In situ stabilization and 2) Ex situ stabilization.

The stabilization technique is not a magic wand that can enhance all soil qualities. The decision to adopt technology is based on which soil characteristics must be altered. Engineers are most curious about soil properties such as volume stability, strength, compressibility, permeability, and durability. Some stabilizing techniques are given below:

a) Mechanical Stabilization b) Stabilization using various types of admixtures

(1) Lime Stabilization

(2) Cement Stabilization

(3) Chemical Stabilization

(4) Fly Ash Stabilization

(5) Rice Husk Ash Stabilization

(6) Bituminous Stabilization

(7) Thermal Stabilization

(8) Electrical Stabilization

(9) Geotextile and Fabric Stabilization

(10) Recycled and Waste Products, and so on. (Afrin, 2017)

1.2 Background of the Study

We can comprehend the significance of soil stabilization by the Pisa Tower, constructed on weak and extremely compressible soils, resulting in leaning instability. (Burland, 2014) It also indicates the incident of the marine drive in Cox's Bazar, Bangladesh, which was exposed to adverse weather conditions, deteriorating the stabilized soil layer and limiting its effectiveness. It was built with inadequate design and testing, and the stabilizer was inappropriate for the soil type. (Cox's Bazar Marine Drive crumbling into sea, 2023) Another event in Dohazari Cox's Bazar train lines also plays a role in understanding the importance of soil stabilization, which was devastated by flood damage. The stabilizer with the rail tracks was not suitable for the soil type. The region's natural water flow and dynamics were not taken into account, resulting in a lack of a comprehensive environmental study. (Sengupta, 2023) All of the mentioned three events lacked a common problem: appropriate soil stabilization.

Figure 1-2 Marine Drive Cox's Bazar

Figure 1-3 Dohazari Cox's Bazar rail tracks

Figure 1-1 Pisa Tower

The transportation facilities and construction projects are the most significant factors for the development of any country. The foundation beds of the infrastructures must be strong for a successful project which requires better soil properties. (Abid, 2016) The key objective of soil stabilization is to enhance the natural soil for the construction of airfields and highways. It also serves to modify the permeability and compressibility of the soil mass in earth structures, regulating the grading of soils and aggregates for the construction of airfield bases and sub-bases, parking lots, site development projects, and numerous other situations where subsoils are unsuitable for construction. Stabilization can be used to treat a broad variety of sub-grade materials, including granular and expansive clays. (Archibong, A REVIEW OF THE PRINCIPLES AND METHODS OF SOIL STABILIZATION, 2020)

1.3 Sandy Soil Issues

Sandy soils can be discovered in a variety of regions of the world. Because of global population increase and urbanization, these soils have been exploited more and more to provide food, feed, fiber, energy, and other services to civilization. The substantial variety can be observed in the physical characteristics of sandy soils (e.g., bulk density, porosity, aggregates) owing to the size and organization of the grains, type of clay, natural processes (e.g., biological activities), or human activities (tillage). (Jingyi Huang∗, Soil and environmental issues in sandy soils, 2020) In the tropical regions, the wet and dry cycles affecting sandy soils are related to seasonality. (Ary Bruand, 2006)

Sandy soils are frequently characterized by high hydraulic conductivity, gas permeability, and specific heat, but low field capacity, permanent wilting point, organic carbon content, and cation exchangeable capacity. Sandy soils have received less research interest than other soil types. (Jingyi Huang∗, Soil and environmental issues in sandy soils, 2020) Sandy soils' physical properties are dominated by their texture. Sandy soils do not aggregate well because of their weak soil structures. Because of its low clay content, sandy soil has comparatively low shrinkage and expansion properties. During the drying process, a loose network with relatively few tiny cracks emerges. Sandy soils demonstrate a wide range of porosity and bulk density. (Osman, 2018)

1.4 Objectives of the Study

- To achieve high soil strength of sandy soils through the mixture of chemical & soil binder stabilization
- To achieve high load-bearing capacity of sandy soils through the mixture of chemical & soil binder stabilization
- To comprehend the strain behavior of sandy soil under the mixture of chemical & soil binder stabilization

1.5 Expected Outcomes

- The Stabilizers will protect sandy soils against landslides and settlement
- The Stabilizers can be utilized in a high-efficiency, and sustainable manner for future construction
- The Stabilizers can be utilized in both shallow and deep foundations for the construction of roads, bridges, airports, dams, high rise buildings etc.

CHAPTER 2
Literature Review

2.1 Importance of soil stabilization

Stabilizing the soil is significant for various reasons. First of all, it increases the soil's ability to support roads, bridges, and buildings by increasing its load-bearing capacity (Khemissa & Mahamedi, 2014). Second, it lessens the permeability of the soil, preventing water infiltration and reducing problems with soil erosion and deterioration (Al-Rawas, Hago, & Al-Sarmi, 2005) (Ingles & Metcalf, 1972). Thirdly, stabilized soil exhibits increased resistance to weathering and environmental changes, contributing to the longevity and safety of engineering projects (Tingle & Santoni, 2003).

2.2 Biological soil stabilization

Plant roots form a network that links soil particles together, strengthening the soil's shear strength and preventing erosion. Plant roots strengthen the soil on slopes, which makes this process very helpful in preventing landslides (H., Gray, B., & Sotir, 1996). Additionally, as it lowers surface runoff velocity and shields the soil's surface from raindrop impacts directly, vegetation is essential in minimizing surface erosion. Because vegetation creates a canopy cover, rainfall has less energy, which minimizes soil dissociation and transport (Morgan, 2009). Also, a newly emerging technique called Microbial-Induced Calcite Precipitation (MICP) involves the use of ureolytic bacteria, such as *Sporosarcina pasteurii*, which hydrolyze urea to produce carbonate ions. These ions react with calcium in the soil to form calcium carbonate, which precipitates and binds soil particles together, thereby increasing soil strength and reducing permeability (DeJong, Mortensen, Martinez, & Nelson, 2010). MICP has been successfully applied in sandy soils to increase their shear strength and reduce liquefaction potential (Cheng & Cord-Ruwisch, 2012).

2.3 Chemical stabilization

In geotechnical engineering, stabilizing soil with chemical admixtures is an essential technique for enhancing soil engineering qualities. Chemical admixtures that improve soil cohesiveness, decrease permeability, and boost soil load-bearing capacity include calcium chloride, sodium silicate, and different polymers. For example, calcium chloride functions by drawing moisture from the atmosphere, which aids in binding soil particles together, enhancing compaction, and lowering dust (Sherwood, 1993). Sodium silicate acts as a chemical grout that forms a gel-like substance, effectively stabilizing sandy soils and reducing water infiltration (Karol, 2003). Polymers, including acrylics and polyvinyl acetates, create a flexible, water-resistant matrix that enhances soil cohesion and erosion resistance, making them effective across different soil types and environmental conditions (Chang, Im, & Cho, 2016).

2.4 Sandy soil behavior under different stabilizers

Sandy soils, which are characterised by high permeability and low cohesiveness, behave differently when stabilized with various substances. In sandy soils, cement works especially well because it creates a cementitious matrix that greatly improves compressive strength and lowers permeability (Consoli, Prietto, & Pasa, 2011). Lime, while more commonly used for clay soils, can still improve workability and reduce shrinkage in sandy soils, though its impact is generally less pronounced (Bell, 1996). The characteristics of sandy soil can be significantly enhanced through the use of chemical stabilizers like sodium silicate and polymers. Sodium silicate works by reducing soil permeability and boosting load-bearing capacity, as it forms a gel-like structure that binds soil particles together, creating a more solid and resilient mass. On the other hand, polymers contribute to soil stabilization by improving cohesion and providing resistance to erosion, as they create a flexible, water-resistant matrix that holds the soil particles in place, offering long-term durability and stability (Chang, Im, & Cho, 2016) (Karol, 2003). These stabilizers are selected based on the specific soil characteristics and engineering needs of a project.

2.5 Usage of stabilized sandy soil

Chemically stabilized sandy soil is widely used in construction projects due to its enhanced mechanical properties, such as increased strength, reduced permeability, and improved durability. Various chemical stabilizers, including cement, lime, and polymers, have been employed to treat sandy soils, making them suitable for applications such as road bases, embankments, and foundations (Al-Rawas & Goosen, 2006). Cement stabilization significantly enhances the compressive strength of sandy soils, making them more durable and resilient under load-bearing conditions. This improved strength reduces the risk of deformation and settlement, ensuring stability and longevity in construction projects such as roads, bridges, and foundations (Shooshpasha & Shirvani, 2015). Polymer stabilizers are increasingly recognized for their effectiveness in minimizing soil erosion and enhancing the cohesion of sandy soils, making them particularly valuable for slope stabilization and erosion control initiatives. Their ability to bind soil particles together creates a more stable and resistant structure, which is crucial in preventing soil displacement in vulnerable areas. However, the success of chemical stabilization with polymers is influenced by various factors, including the specific soil characteristics, the choice of stabilizer, and prevailing environmental conditions. These factors must be meticulously evaluated during the design and application stages to ensure optimal performance and long-term stability (Latifi, Aminaton, Rashid, & Yii, 2016) (Bell, 1996). Overall, chemically stabilized sandy soils have proven to be a versatile and effective solution in various construction scenarios, offering improved performance and longevity of the constructed structures.

CHAPTER 3
Methodology

3.1 Introduction

The thesis investigates the behavior of sandy soil resulting in stabilization with a chemical and soil binder mixture in terms of its maximum strength and load-bearing capacity. The goal is to determine if the treated soil is practicable for use in constructing roads, highways, buildings, and other structures. A sequential approach was implemented from the initial phase of sample collection to the assessment of treated soil parameters. The figure below depicts the flowchart of the process step by step:

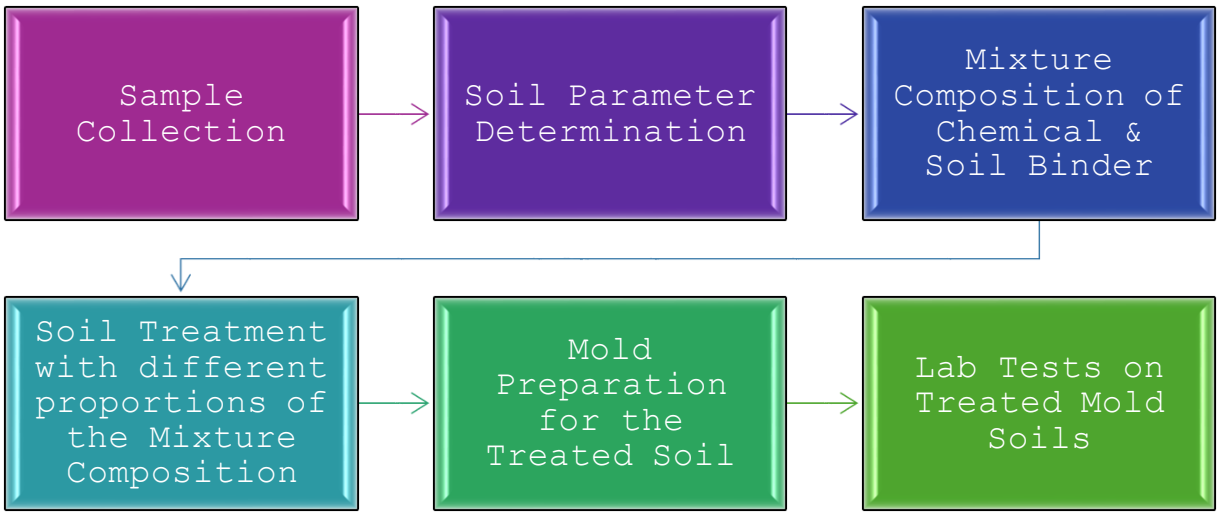

Figure 3-1 Flow-Chart process of Methodology

3.2 Sample Collection

3.2.1 Sandy Soil

Sandy soil samples were collected near our university campus during a construction project. We had purchased around 10 kilograms of river sandy soils.

Figure 3-2 Sandy Soil

3.2.2 Chemical (TX-95)

The chemical was safely collected from the representative of PRECIOUS ROAD ENGINEERING MANAGEMENT through our supervisor.

Figure 3-3 Soil Binder (SB-95)

3.2.3 Soil Binder (SB-95)

The soil binder was safely received from the representative of PRECIOUS ROAD ENGINEERING MANAGEMENT through our supervisor.

Figure 3-4 SB-95

Address:

NEW NO.42, (OLD NO.31)

PURAM PRAKASHAM STREET,

BALAJI NAGAR, ROYAPETTAH,

CHENNAI – 60001

Phone: +91 7903839574

EMAIL: info@preciousprem.com

3.3 Soil Parametre Determination

The general soil parameters of a sample are assessed through lab experiments. We've conducted the lab tests to better understand the soil characteristics of our sample. The following experiments were undertaken to determine soil parameters: Sieve analysis, hydrometer analysis, specific gravity tests, compaction tests, permeability tests, direct shear tests, CBR tests, and relative density tests. All the tests were conducted according to ASTM standards.

3.3.1 Sieve Analysis

Table 3-1 Experimental Data of Sieve Analyis

Sieve No.	Sieve Opening (mm)	Wt. of Sieve (gm)	Wt. of Sieve+Soil (gm)	Wt. of soil Retained (gm)	% of Soil Retained	Cumulative % Retained	% Finer
#4	4.75	335.63	335.65	0.02	0.004	0.004	99.996
#8	2.36	326.56	326.73	0.17	0.034	0.038	99.962
#16	1.18	314.75	315.06	0.31	0.062	0.1	99.9
#30	0.6	313.4	313.86	0.46	0.092	0.192	99.808
#150	0.3	302.3	304.31	2.01	0.402	0.594	99.406
#100	0.15	295.5	478.985	183.485	36.697	37.291	62.709
#200	0.075	288.65	560.15	271.5	54.3	91.591	8.409
Pan		213.6	254.87	41.27	8.254	99.845	**0.155**

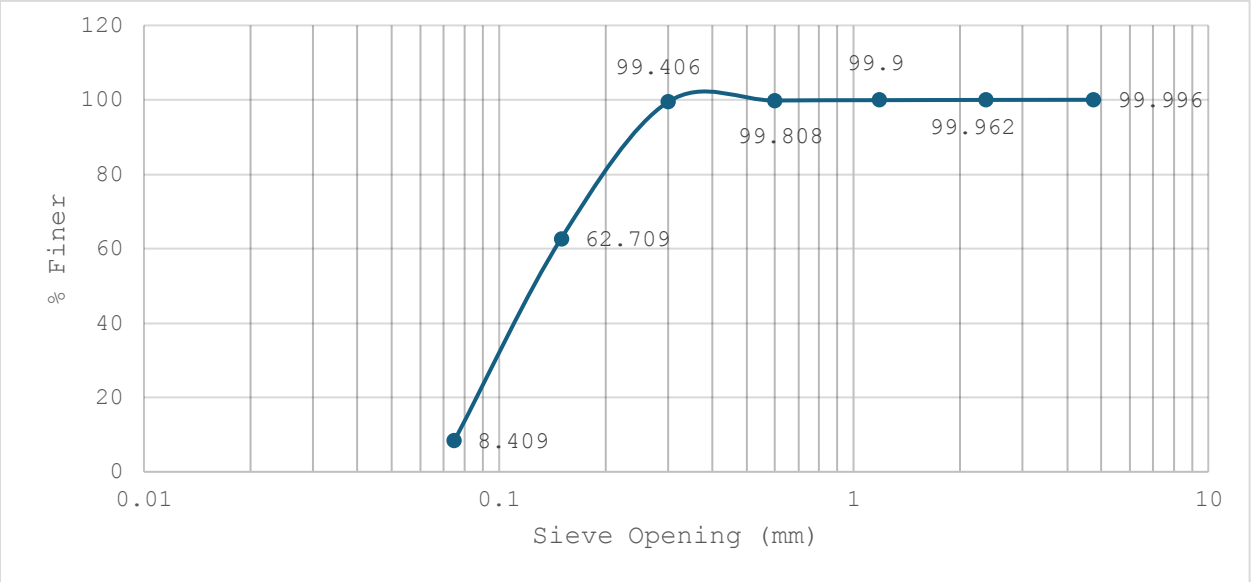

Figure 3-5 Graph showing trendline of %Finer after Sieve Opening upto 0.075 mm

3.3.2 Hydrometre Analysis

Table 3-2 Experimental Data of Hydrometre Analyis

Elapsed time, t (min)	Room Temp. (C)	Actual Hydro Rdg, R_a	Reading after meniscus correction, $R = R_a - C_m$	Effective Depth, L (cm)	Value of K	D in mm = $k\sqrt{L/t}$	C_t	a	Corrected Hydrometre Reading, $R_c = R_a - C_z \pm C_t$	Percent Finer = $R_c * a / W_s$
0.25	27	10.5	9.5	14.6	0.013	0.2002201	2	1.03	7.5	3.0714285
0.5		6	5	15.704	0.013	0.1038260	2	1.03	8	3.2761904
1		5	4	16.3	0.013	0.0528889	2	1.03	7	2.8666666
2		4	3	15.6	0.013	0.0258704	2	1.03	6	2.4571428
4		4	3	15.6	0.013	0.0129352	2	1.03	6	2.4571428
8		3.5	2.5	15.7	0.013	0.0064883	2	1.03	5.5	2.2523809
15		3.5	2.5	15.7	0.013	0.0034604	2	1.03	5.5	2.2523809
30		3.25	2.25	15.75	0.013	0.0017329	2	1.03	5.25	2.15
60		3	2	15.8	0.013	0.0008678	2	1.03	5	2.0476190
120		3	2	15.8	0.013	0.0004339	2	1.03	5	2.0476190
240		2.5	1.5	15.9	0.013	0.0002176	2	1.03	4.5	1.8428571
480		2.5	1.5	15.9	0.013	0.0001088	2	1.03	4.5	1.8428571
1440		2.5	1.5	15.9	0.013	3.627E-05	2	1.03	4.5	1.8428571

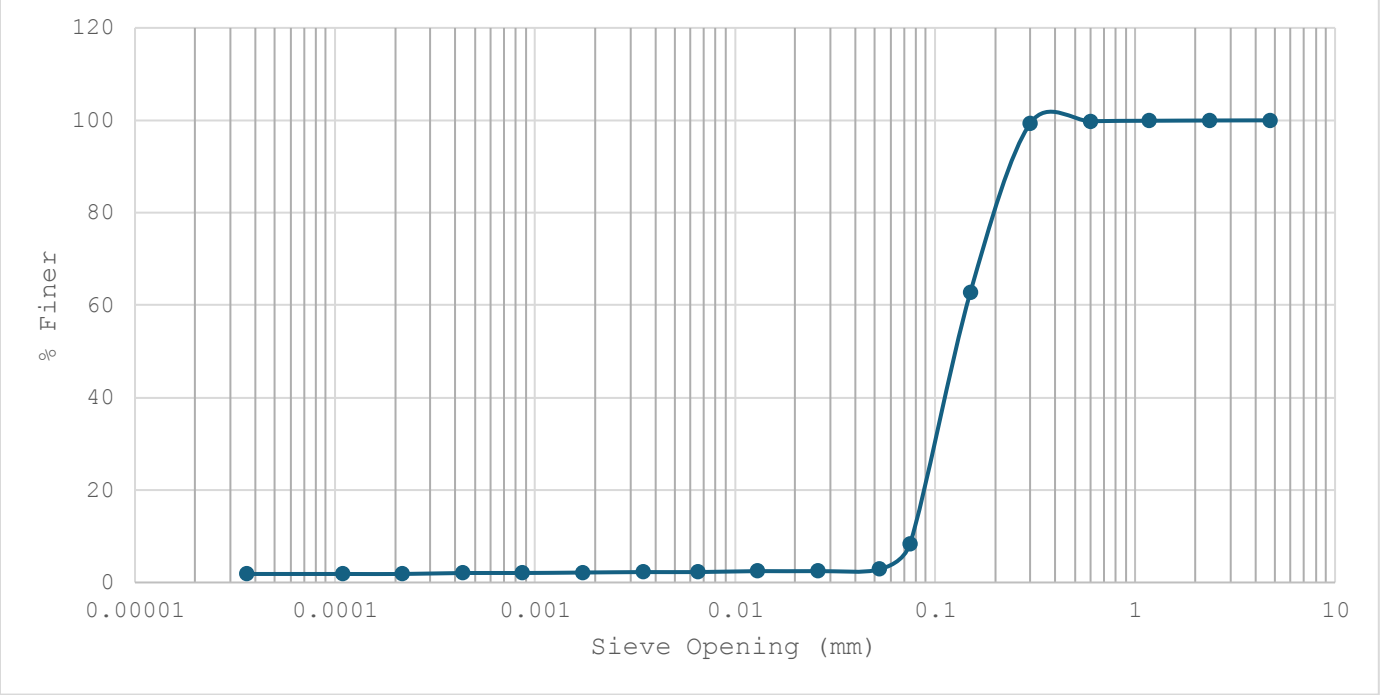

Figure 3-6 Graph showing trendline of %Finer after Sieve Opening including fine particles <0.075 mm

According to the Unified Soil Classification System (ASTM D 2487), gravels are materials that pass through a 75 mm sieve but are retained on a 4.75 mm sieve. Sand represents the materials that pass through a 4.75 mm sieve and are retained at 0.075 mm. Materials passing through 0.075 mm that demonstrate plasticity and strength when dry is clay, whereas those that are non-plastic yet have minimal strength when dry is silt. (ASTM Aggregate and Soil Terminology, n.d.) Sand particles are the most prevalent in our soil sample composition.

Table 3-3 Soil Content of the Sample

Soil Type	Percentage (%)
Gravel	0.004
Sand	99.841
Silt & Clay	0.155

3.3.3 Specific Gravity Test

Table 3-4 Experimental Data of Specific Gravity Test

Wt. of Dry Soil, W_s (gm)	Wt. of Pycnometre + Water = W_1 (gm)	Temperature of Water, °C	Wt. of Pycnometre + Water + Soil = W_2 (gm)	Wt. of equal volume of water as the soil solids , $W_w=W_1+W_s-W_2$	Specific Gravity of Water = G_T at T°C	G_s at T°C = (W_s/W_w) *G_T
50	354.68	30	384.9	19.78	0.9974	**2.52**

In sandy soils, the normal range of specific gravity for road construction is 2.5-3. (Siddiquee, n.d.)The value of our sandy soil sample is within the typical range, indicating that it is suitable for road construction.

3.3.4 Compaction Test

Table 3-5 Experimental Data of Compaction Test

Sample No.	Can No.	Wt. of Can (kg)	(Wt. of Can+ Wet soil) kg	(Wt. of Can + Dry Soil) kg	Wt. of Dry Soil (kg)	Wt. of Moisture (kg)	Moisture Content (%)
1	3	0.026	0.071	0.069	0.043	0.045	2.5
2	55	0.029	0.069	0.067	0.038	0.04	5
3	125	0.046	0.086	0.084	0.038	0.04	7.5
4	21	0.027	0.071	0.067	0.04	0.044	10
5	53	0.033	0.079	0.067	0.034	0.046	**12.5**
6	133	0.027	0.061	0.055	0.028	0.034	15

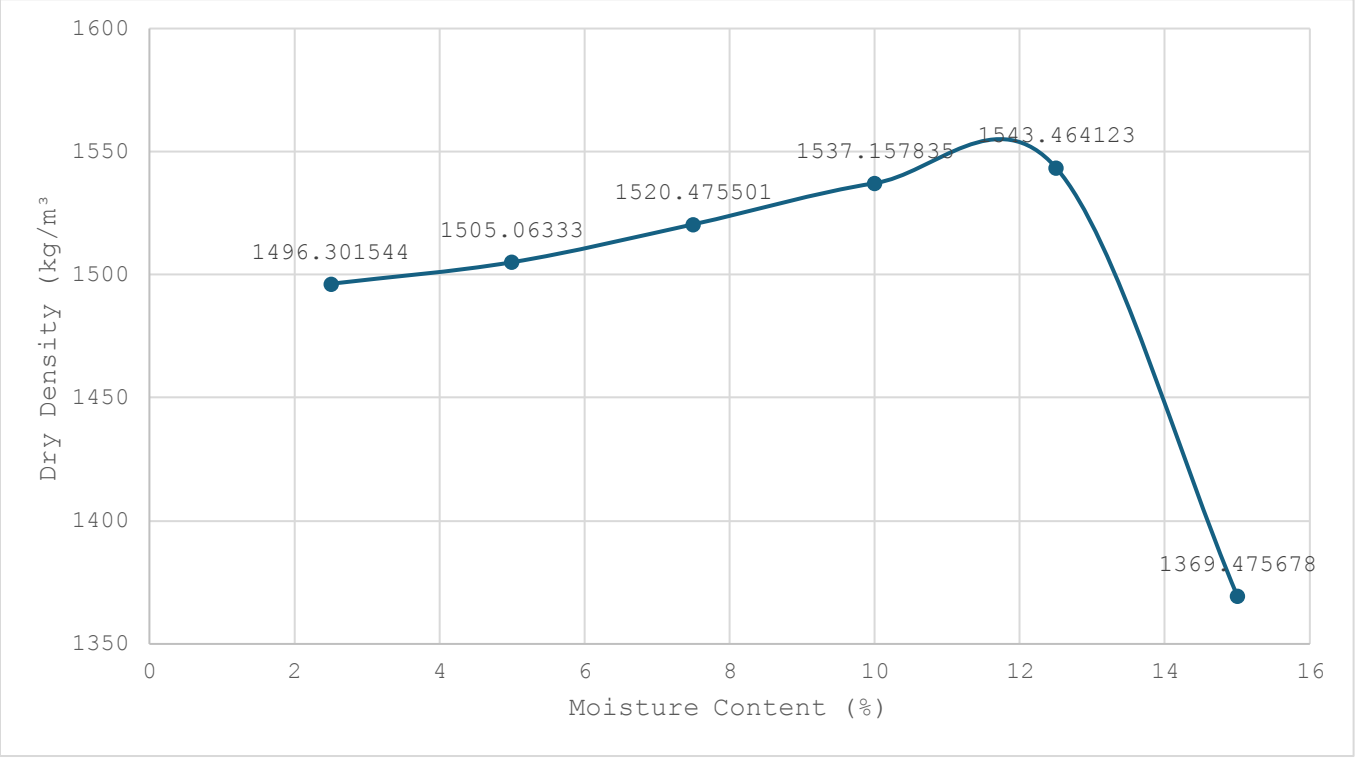

Figure 3-7 Graph showing trendline of dry density with respect to moisture content

The above trendline demonstrates that the optimum moisture content is **12.5%**. Engineers must achieve a compaction level between 90% and 95% of the maximum dry density while constructing highway embankments, earth dams, and other engineering structures. (Arinze, 2014)

Table 3-6 Experimental Data of Compaction Test

Wt. of Mold (kg)	(Wt. of Mold + Compacted Soil) kg	Wt. of Compacted Soil (kg)	Wet Density	Dry Density	Void Ratio, e
4.234	5.649	1.415	1533.70908	1496.301544	0.68497692
4.234	5.692	1.458	1580.3165	1505.06333	0.67516776
4.234	5.742	1.508	1634.51116	1520.475501	0.65818756
4.234	5.794	1.56	1690.87362	1537.157835	0.64019173
4.234	5.836	1.602	1736.39714	1543.464123	0.63349023
4.234	5.687	1.453	1574.89703	1369.475678	0.84102106

The void ratio is determined using this formula considering the relative density as 90% due to field compaction. (Das, 2006)

$$D = \frac{e_{max} - e}{e_{max} - e_{min}} \times 100\%$$

The void ratio of our sample is 0.651. Finally, the dry unit weight is obtained from the void ratio using this formula. (Das, 2006)

$$\gamma_d = \frac{W_S}{V} = \frac{G_S \gamma_W}{1 + e}$$

The dry unit weight of the soil is 16.431 kN/m^3.

3.3.5 Direct Shear Test

In order to calculate internal friction based on field conditions, the direct shear sample was compacted using a dry unit weight of 16.431 kN/m^3. The sample diameter is 63 mm. The Calibration factor of the testing machine is 1.0017N-0.3285

Table 3-7 Experimental Data of Direct Shear Test

Normal Load (kg)	1	2	3
Sample Depth (mm)	26.37	26.27	25.81
Wt. of Dry Sample (gm)	134.4	134	131.64

Table 3-8 Shear Stress Data for 1 kg

Normal Load = 1 kg					
Elapsed Time	Shear Displacement (mm)	Normal Displacement Dial (mm)	Load Cell Reading (N)	Shear Force (kg)	Shear Stress (kg/sq mm)
15 sec	0.26	-0.05	4	3.6783	1.179
30 sec	0.516	-0.059	17	16.7004	5.357
45 sec	0.771	-0.023	32	31.7259	10.177
1 min	1.046	0.022	43	42.7446	13.712
1:15	1.26	0.103	52	51.7599	16.604
1:30	1.61	0.225	63	62.7786	20.139
1:45	1.95	0.335	61	60.7752	19.496
2 min	2.3	0.426	58	57.7701	18.532
2:15	2.6	0.486	41	40.7412	13.069
2:30	2.94	0.538	32	31.7259	10.177

Table 3-9 Shear Stress Data for 2 kg

Normal Load = 2 kg					
Elapsed Time	Shear Displacement (mm)	Normal Displacement Dial (mm)	Load Cell Reading (N)	Shear Force (kg)	Shear Stress (kg/sq m)
15 sec	0.17	-0.113	12	11.6919	3.7507
30 sec	0.36	-0.11	23	22.7106	7.285
45 sec	0.65	-0.093	49	48.7548	15.6403
1 min	0.94	-0.048	71	70.7922	22.709
1:15	1.19	-0.007	94	93.8313	30.1006
1:30	1.51	0.069	107	106.8534	34.278
1:45	1.92	0.162	125	124.884	40.062
2 min	2.19	0.207	118	117.8721	37.812
2:15	2.43	0.233	96	95.8347	30.743
2:30	2.75	0.246	82	81.8109	26.244

Table 3-10 Shear Stress Data for 3 kg

Normal Load = 3 kg					
Elapsed Time	Shear Displacement (mm)	Normal Displacement Dial (mm)	Load Cell Reading (N)	Shear Force (kg)	Shear Stress (kg/sq m)
15 sec	0.169	-0.267	32	31.7259	10.177
30 sec	0.391	-0.286	63	62.7786	20.139
45 sec	0.58	-0.286	78	77.8041	24.959
1 min	0.82	-0.269	97	96.8364	31.064
1:15	1.05	-0.243	119	118.8738	38.134
1:30	1.29	-0.178	137	136.9044	43.918
1:45	1.47	-0.129	156	155.9367	50.023
2 min	1.74	-0.064	176	175.9707	56.4505
2:15	2.04	-0.011	188	187.9911	60.306
2:30	2.35	0.084	161	160.9452	51.6304
2:45	2.5	0.129	143	142.9146	45.846
3 min	2.95	0.172	119	118.8738	38.134

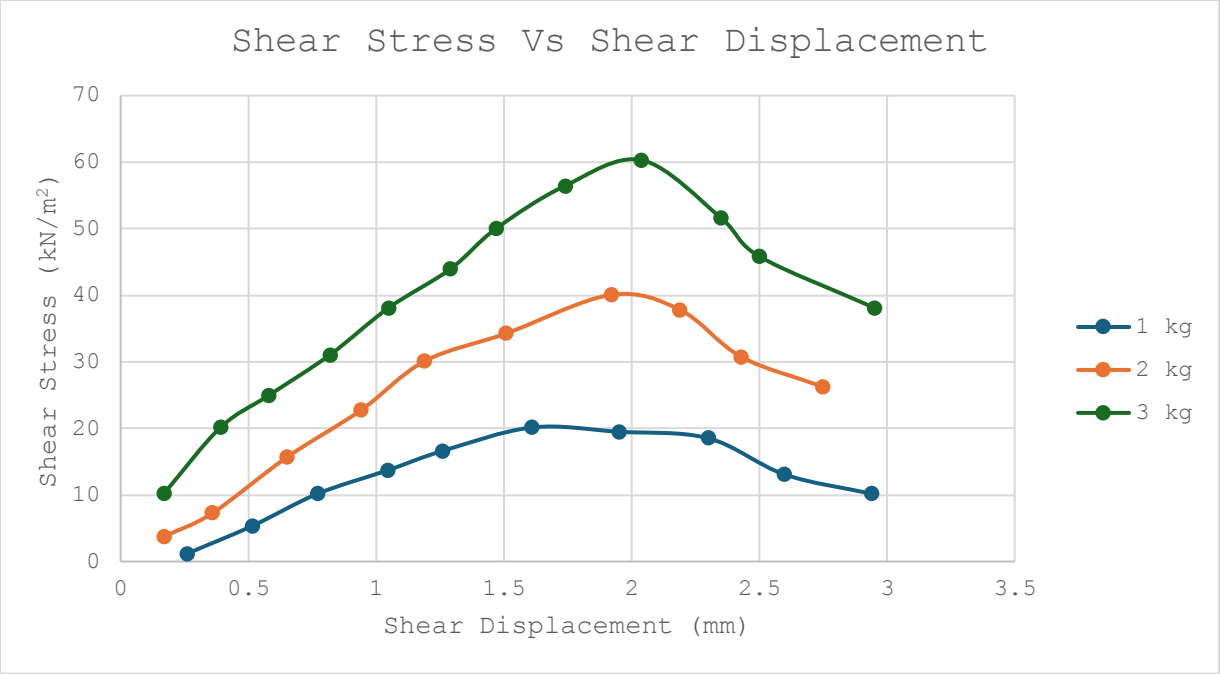

Figure 3-8 Graph showing trendline of shear displacement (mm) with respect to shear stress (kN/m^2)

Table 3-11 Shear Stress and Normal Stress Data

Normal Load (kg)	Normal Stress (kN/sq m)	Maximum Shear Stress (kN/sq m)
1	31.458	20.139
2	62.917	40.062
3	94.376	60.306

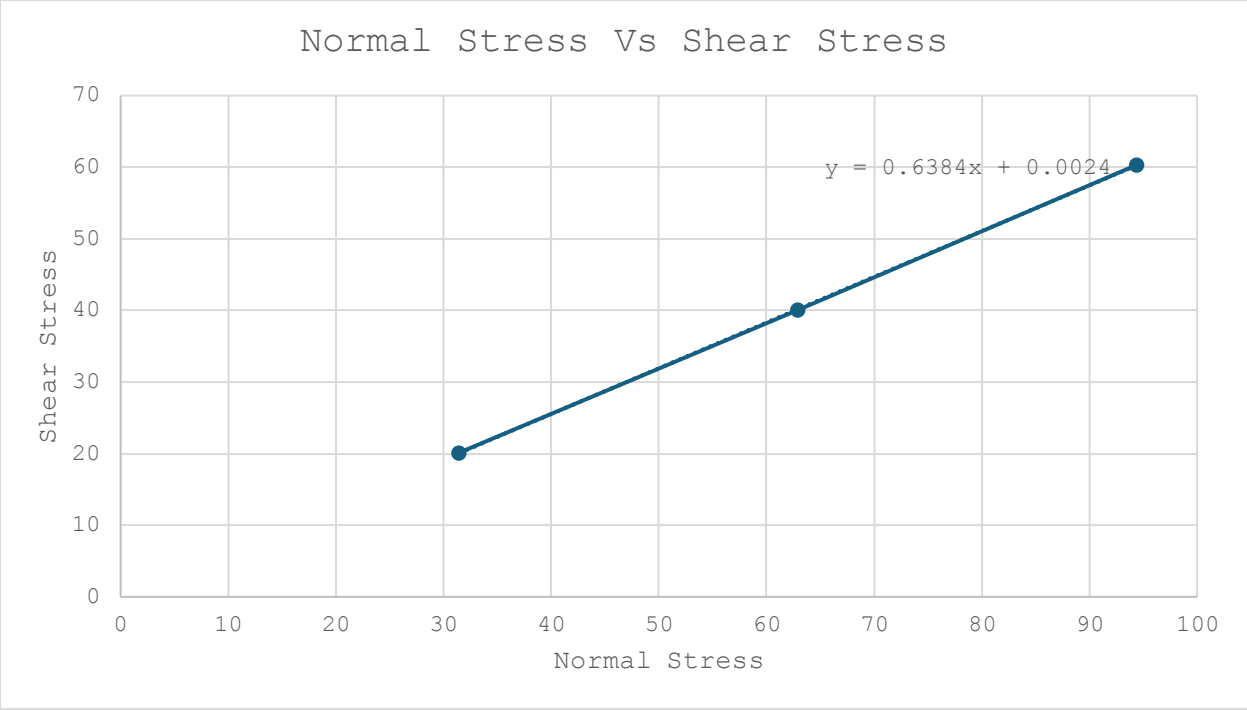

Figure 3-9 Graph showing trendline of shear stress (kN/m^2) with respect to normal stress (kN/m^2)

There were no fine particles present in the sample, as indicated by the sample's cohesion of -0.002 The sample has an internal friction angle of 32.55°, which implies our soil sample is well-graded loose sands with angular grains. (Friction Angle of Soils + Typical Values, n.d.)

3.3.6 Permeability Test

Table 3-12 Experimental Data of Permeability Test

Test No.	1	2	3
Average Flow, Q (cm^3)	500	700	1000
Time of Collection, t (s)	61 s	241 s	329 s
Temperature of water, T (°C)	30	30	30
Head Difference, h (cm)	103	103	103
Diametre of Specimen, D (cm)	7.8	7.8	7.8
Length of Specimen, L (cm)	20.5	20.5	20.5
Area of Specimen, A = ¼*π*D^2 (cm^2)	47.783736	47.783736	47.783736
$k = \frac{QL}{Aht}$ (cm/s)	0.03414104	0.0120981	0.0126602
Average k (cm/s)	0.019633116		
$k_{20} = k_T \frac{\eta_T}{\eta_{20}}$ (cm/s)	**1.56E-3**		

The soil sample has a permeability of 1.56E-3 cm/s. Our sample is clean sand since the normal values of clean sand vary from 1.00E-5 to 1.00E-2 cm/s. (Soil permeability coefficient, 2013)

3.3.7 Relative Density Test

The height and diameter of the sample is 6.1 inch and 6 inches respectively. The dry unit weight of the soil in its natural state is 92 pcf.

Table 3-13 Loosest State Data

Loosest State (min)					
No. of Observations	Wt. of mold + Soil (lb)	Wt. of mold (lb)	Wt. of Soil (lb)	Density (pcf)	Average Density (pcf)
1	28.263	20.646	7.617	76.31404276	76.08360781
2	28.197	20.646	7.551	75.65279465	
3	28.26	20.646	7.614	76.28398602	

Table 3-14 Reduced Volume Data

Sample	Height (inch)	Reduced Volume
1	4.8584	0.07949557
2	4.833	0.079079963
3	4.743	0.077607338

Table 3-15 Densest State Data

Densest State (max)					
No. of Observations	Wt. of mold + Soil (lb)	Wt. of mold (lb)	Wt. of Soil (lb)	Density (pcf)	Average Density (pcf)
1	28.263	20.646	7.617	95.81665997	96.47052314
2	28.197	20.646	7.551	95.4856295	
3	28.26	20.646	7.614	98.10927994	

The Relative density of the soil is 81.865%. The sample belongs in the dense sand category. (Sivakugan, 2006)

3.3.8 California Bearing Ratio Test (Unsoaked)

The Calibration factor of the testing machine is 0.04219D with 56 number of blows per layer. The Optimum moisture content (12.5%) was applied during the test. The sample dimensions are:

Inner Diameter of Sample = 6 inch

Height of Mold = 7 inch

Height of Disc = 2.416 inch

Height of Sample = 4.584 inch

Table 3-16 Sample 1 Data

Sample 1 (Can No. 16)	
Weight of Mold (kg)	6.078
Weight of Sample + Mold (kg)	17.768
Weight of Sample (kg)	11.69
Weight of Can	18.82
Weight of Can + Wet Soil	57.84
Weight of Can + Dry Soil	53.98

Table 3-17 Sample 1 Penetration Reading Data

Sample 1					
Penretration Reading	Penetration (inch)	Proving Ring Dial	Load (kN)	Load (lb)	Stress (kN/m²)
50	0.025	8.5	0.3587	80.63896678	19.6634141
100	0.05	23.5	0.9917	222.9430258	54.36355663
150	0.075	42.5	1.7935	403.1948339	98.3170705
200	0.1	62.5	2.6375	592.9335793	144.5839272
250	0.125	78.5	3.3127	744.7245755	181.5974126
300	0.15	92.5	3.9035	877.5416973	213.9842123
350	0.175	98	4.1356	929.7198523	226.7075979
400	0.2	99.75	4.20945	946.3219925	230.7559478

Table 3-18 Sample 2 Data

Sample 2 (Can No. 53)	
Weight of Mold (kg)	6.609
Weight of Sample + Mold (kg)	18.266
Weight of Sample (kg)	11.657
Weight of Can	32.82
Weight of Can + Wet Soil	61.58
Weight of Can + Dry Soil	58.5

Table 3-19 Sample 2 Penetration Reading Data

Sample 2					
Penretration Reading	Penetration (inch)	Proving Ring Dial	Load (kN)	Load (lb)	Stress (kN/m²)
50	0.025	14	0.5908	132.8171218	32.38679969
100	0.05	30	1.266	284.608118	69.40028506
150	0.075	46	1.9412	436.3991143	106.4137704
200	0.1	61	2.5742	578.7031733	141.1139129
250	0.125	76	3.2072	721.0072324	175.8140555
300	0.15	87	3.6714	825.3635423	201.2608267
350	0.175	95	4.009	901.2590405	219.7675693
400	0.2	97	4.0934	920.232915	224.394255

Table 3-20 Sample 3 Data

Sample 3 (Can No. 141)	
Weight of Mold (kg)	6.612
Weight of Sample + Mold (kg)	18.284
Weight of Sample (kg)	11.672
Weight of Can	28.39
Weight of Can + Wet Soil	58.4
Weight of Can + Dry Soil	55.26

Table 3-21 Sample 3 Penetration Reading Data

Sample 3					
Penretration0 Reading	Penetration (inch)	Proving Ring Dial	Load (kN)	Load (lb)	Stress (kN/m²)
50	0.025	15	0.633	142.304059	34.70014253
100	0.05	32	1.3504	303.5819926	74.02697073
150	0.075	46	1.9412	436.3991143	106.4137704
200	0.1	59	2.4898	559.7292988	136.4872273
250	0.125	71	2.9962	673.572546	164.2473413
300	0.15	80	3.376	758.9549814	185.0674268
350	0.175	84	3.5448	796.9027305	194.3207982
400	0.2	95	4.009	901.2590405	219.7675693

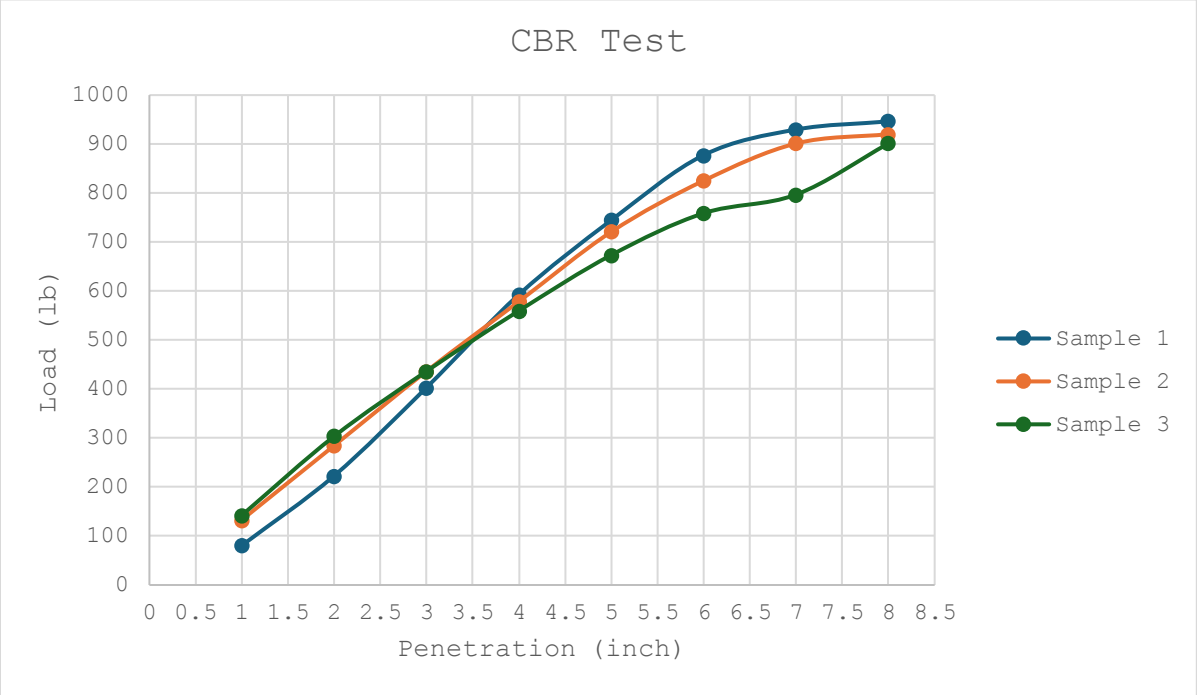

Figure 3-10 Graph showing trendline of load (lb) with respect to penetration (inch)

The CBR value of a sample is determined between load (kN) @ 0.1″ and 0.2″ with respect to 13.44 kN and 20.06 kN respectively. Between the three samples, the CBR value is 20.984%, which is within the typical range for sandy soil. (Jones, 2017)

3.4 Mixture Composition of Chemical (TX-95) & Soil Binder (SB-95)

Under the guidelines provided by the company representatives at the beginning of the project, a trial mixture was produced, with 5.5% SB-95 (based on soil weight), OMC and 0.65 kg/m^3 soil TX-95 for low plasticity soils (PI<20). Based on our soil content, sand is predominant, indicating low plasticity. The sample broke after being removed from the mold using a hydraulic jack after it had completely dried, indicating that it had not gained adequate strength. The identical case followed the second trial mixture composition produced with 6.5% SB-95 (based on soil weight), OMC, and 0.75 kg/m^3 soil TX-95. The third trial was conducted with 7.5% SB-95 (based on soil weight), OMC, and 0.75 kg/m^3 soil TX-95. The sample began to acquire strength in the third trial, although it was still effortlessly breakable. In the final discussions, we had agreed to raise the TX-95 concentration to 1.3 kg/m^3 of soil. Subsequently, the sample is completely ready for testing.

Table 3-22 Mixture Composition of different trials

Trial No.	SB-95 %	TX-95	Sample State
1	5.5	0.65 kg/m^3	Broken
2	6.5	0.75 kg/m^3	Broken
3	7.5	0.75 kg/m^3	Strength Gained but Easily Breakable
4	7.5	1.3 kg/m^3	Ready for Test

Figure 3-11 Samples of Trial-1,2 & 3

3.5 Soil Treatment with different proportions of the Mixture Composition

Following the trial combination consisting of 7.5% SB-95 (based on soil weight), OMC, and 0.75 kg/m^3 soil TX-95, we produced further mixture compositions with 10%, 12.5%, and 15% SB-95 while maintaining a constant TX-95 concentration of 1.3 kg/m^3 soil. The TX-95 content was kept constant because it demonstrated that the sample had developed to adequate strength and that the SB-95 content's performance could be evaluated clearly according to the TX-95 content.

3.5.1 Sample Calculation of the Mixture Composition

A sample calculation for 5 kg soil is shown in the following table.

Table 3-23 Sample Calculation of mixture composition for 5 kg Soil

% of mixture	TX-95 (kg per m^3 soil)	SB-95 (gm)	TX-95 (gm)	Optimum Moisture Content (12.5%) (mL)
7.5	1.3	375	3.97	625
10		500	3.97	625
12.5		625	3.97	625
15		750	3.97	625

7.5% SB-95 of 5 kg Soil = $500 \times \frac{7.5}{100}$ = 375 gm

1.3 kg/m^3 soil TX-95, $V = \frac{W}{K} = \frac{5\ kg}{16.043\ kN/m^3} = \frac{5 \times 9.81}{16.431 \times 1000}$ = 3.057E-3 m^3

TX-95 (gm) for 5 kg Soil = 3.057E-3×1.3×1000 = 3.97 gm

12.5% OMC (mL) required for 5 kg soil = $12.5 \times \frac{5000}{100}$ = 625 mL

3.5.2 Mixing Procedure

Initially, the soil sample was brought into the laboratory. A solution was prepared using the TX-95 content and the optimum moisture content required for the weight of the soil sample after the mixture composition was calculated. The sample soil and the required SB-95 content were combined using our bare hands. The solution was gradually poured into the mixed sample soil for the final combination.

Figure 3-12 Mixing TX-95 with OMC

Figure 3-13 Mixing SB-95 with Soil Sample

Figure 3-14 Final Mixture

3.6 Mold Preparation for the Treated Soil

Following the completion of the mixture, we created molds for every percentage composition of the mixture that required to be tested at 3, 7, 14, and 28 days of curing time to ensure the accuracy of the results.

Two molds have been developed in preparation for each curing day's Unconfined Compressive Strength and California Bearing Ratio tests. For testing, a total of 32 molds have been created by us.

3.6.1 Preparation of UCS molds

For compaction, we've placed the treated soil into several UCS molds. A 2.5 kg rammer dropped from a height of 305 mm compressed the mixture with 25 blows in 3 layers. (MD Sahadat Hossain, Islam, Badhon, & Imtiaz, 2021) The molds were safely kept in the sun to dry out after compaction.

Figure 3-15 UCS Molds kept for drying

Figure 3-16 UCS samples removing from molds

3.6.2 Preparation of CBR molds

The CBR molds were filled with the treated soil for the compaction. The mixture was compacted with 56 blows in 3 layers of a 2.6 kg rammer dropped from 305 mm height. (Mane, 2020) The molds were safely kept under the sun after the compaction for getting completely dried.

Figure 3-17 CBR Molds

3.7 Lab Tests on Treated Mold Soil

The molds were prepared to measure the compressive strength of the stabilized soil without any lateral confinement and assess the strength of stabilized soils whether it can be applied as a subgrade soil in the design of pavements and highways. That's why, we've conducted the Unconfined Compressive Strength test & California Bearing Ratio test for every molds.

3.7.1 Lab Apparatus

Figure 3-18 UCS test

Figure 3-19 CBR test

3.7.2 Sample Preparation for UCS test

The mold samples were trimmed following the length double of the diameter and ensured the ends of the sample are flat and perpendicular to the axis. (MD Sahadat Hossain, Islam, & Fahim, Properties and Behavior of Soil – Online Lab Manual, 2021) After that, the trimmed sample was place on the machine to be prepared for the test. The Unconfined Compressive Strength test was conducted according to ASTM D2166 Standard. We've conducted the UCS test to observe the maximum compressive strength that the stabilized soil will be able to undertake.

Figure 3-20 Trimmed Sample of UCS test

3.7.3 Sample Preparation for CBR test

The California Bearing Ratio test was conducted according to ASTM D1883 Standard. A Surcharge of 4.54 kg weight was placed on top of the mold sample. Then, the mold was placed on the machine to be prepared for the test. We've conducted the unsoaked CBR test to observe the maximum load that the stabilized soil can support.

CHAPTER 4
Results & Discussions

The laboratory test results of the Unconfined Compressive Strength test & California Bearing Ratio test of the treated soil shows the ability of the stabilizers to be applied in the real field conditions in constructing highways, pavements, foundation of high-rise structures etc. The test results are shown below:

4.1 Unconfined Compressive Strength Test

The Calibration factor of the Unconfined Compressive Strength test is 1.0132D

4.1.1 7.5% Mixture Composition

The diameter of the trimmed sample is 39 mm and the length of the sample is 75 mm for 3 days curing period.

Table 4-1 UCS test data of 3 days

load dial	calibrated (kg)	displacement dial gauge reading	unit strain L_0/L	corrected $A=A_0/(1-(L_0/L))$	stress Kg/mm^2	stress N/mm^2
0.3	0.30396	0.1	0.13%	1196.188318	0.000254107	0.00249025
0.7	0.70924	0.2	0.27%	1197.7875	0.000592125	0.005802826
1.2	1.21584	0.3	0.40%	1199.390964	0.001013714	0.009934402
2.3	2.33036	0.4	0.53%	1200.998727	0.001940352	0.019015447
3.5	3.5462	0.5	0.67%	1202.610805	0.002948751	0.028897761
4.1	4.15412	0.6	0.80%	1204.227218	0.003449615	0.033806225
5.2	5.26864	0.7	0.93%	1205.847981	0.004369241	0.042818558
6.3	6.38316	0.8	1.07%	1207.473113	0.005286379	0.05180651
7.8	7.90296	0.9	1.20%	1209.102632	0.006536219	0.064054949
8.5	8.6122	1	1.33%	1210.736554	0.007113191	0.069709269
9.4	9.52408	1.2	1.60%	1214.017683	0.007845092	0.076881898
7.3	7.39636	1.4	1.87%	1217.316644	0.006075954	0.05954435
2.1	2.12772	1.6	2.13%	1220.633583	0.001743128	0.01708265

The diameter of the trimmed sample is 36.76 mm and the length of the sample is 71 mm for 7 days curing period.

Table 4-2 UCS test data of 7 days

load dial	calibrated (kg)	displacement dial gauge reading	unit strain L_0/L	corrected $A=A_0/(1-(L_0/L))$	stress Kg/mm^2	stress N/mm^2
1.1	1.11452	0.1	0.14%	1062.806045	0.001048658	0.010276848
1.8	1.82376	0.2	0.28%	1064.307183	0.001713565	0.016792941
2.4	2.43168	0.3	0.42%	1065.812568	0.002281527	0.022358963
2.7	2.73564	0.4	0.56%	1067.322218	0.002563087	0.025118255
3.1	3.14092	0.5	0.70%	1068.83615	0.002938636	0.028798629
3.6	3.64752	0.6	0.85%	1070.354383	0.003407769	0.033396132
9.9	10.03068	0.7	0.99%	1071.876936	0.009358052	0.091708909
13.8	13.98216	0.8	1.13%	1073.403826	0.013026002	0.127654816
16.8	17.02176	0.9	1.27%	1074.935073	0.015835152	0.155184487
19.2	19.45344	1	1.41%	1076.470694	0.0180715	0.177100699
20	20.264	1.2	1.69%	1079.555137	0.018770695	0.183952809
20.4	20.66928	1.4	1.97%	1082.657307	0.019091249	0.187094238
18.1	18.33892	1.6	2.25%	1085.777357	0.016890129	0.165523268

The diameter of the trimmed sample is 39 mm and the length of the sample is 75 mm for 14 days curing period.

Table 4-3 UCS test data of 14 days

load dial	calibrated (kg)	displacement dial gauge reading	unit strain L_0/L	corrected $A=A_0/(1-(L_0/L))$	stress Kg/mm^2	stress N/mm^2
2	2.0264	0.1	0.13%	1196.188318	0.001694048	0.016601667
4.3	4.35676	0.2	0.27%	1197.7875	0.00363734	0.035645929
7.9	8.00428	0.3	0.40%	1199.390964	0.00667362	0.06540148
18.8	19.04816	0.4	0.53%	1200.998727	0.015860267	0.155430613
28.8	29.18016	0.5	0.67%	1202.610805	0.024264009	0.237787293
35.44	35.907808	0.6	0.80%	1204.227218	0.029818134	0.292217709
34.6	35.05672	0.7	0.93%	1205.847981	0.029072255	0.284908099
34	34.4488	0.8	1.07%	1207.473113	0.028529662	0.279590689
33.5	33.9422	0.9	1.20%	1209.102632	0.028072224	0.275107796
32.9	33.33428	1	1.33%	1210.736554	0.027532232	0.269815876
30	30.396	1.2	1.60%	1214.017683	0.025037527	0.24536776

The diameter of the trimmed sample is 39 mm and the length of the sample is 75 mm for 28 days curing period.

Table 4-4 UCS test data of 28 days

load dial	calibrated (kg)	displacement dial gauge reading	unit strain L_0/L	corrected $A=A_0/(1-(L_0/L))$	stress Kg/mm^2	stress N/mm^2
0.9	0.91188	0.1	0.13%	1196.188318	0.000762321	0.00747075
1.4	1.41848	0.2	0.27%	1197.7875	0.00118425	0.011605651
2.8	2.83696	0.3	0.40%	1199.390964	0.002365334	0.023180271
9.3	9.42276	0.4	0.53%	1200.998727	0.00784577	0.076888548
11.3	11.44916	0.5	0.67%	1202.610805	0.009520254	0.093298487
15.9	16.10988	0.6	0.80%	1204.227218	0.013377774	0.131102189
21.3	21.58116	0.7	0.93%	1205.847981	0.017897082	0.175391402
27.6	27.96432	0.8	1.07%	1207.473113	0.023159373	0.226961854
31.2	31.61184	0.9	1.20%	1209.102632	0.026144877	0.256219798
37.9	38.40028	1	1.33%	1210.736554	0.031716462	0.310821328
40.4	40.93328	1.2	1.60%	1214.017683	0.033717202	0.330428584
36.3	36.77916	1.4	1.87%	1217.316644	0.030213306	0.296090397

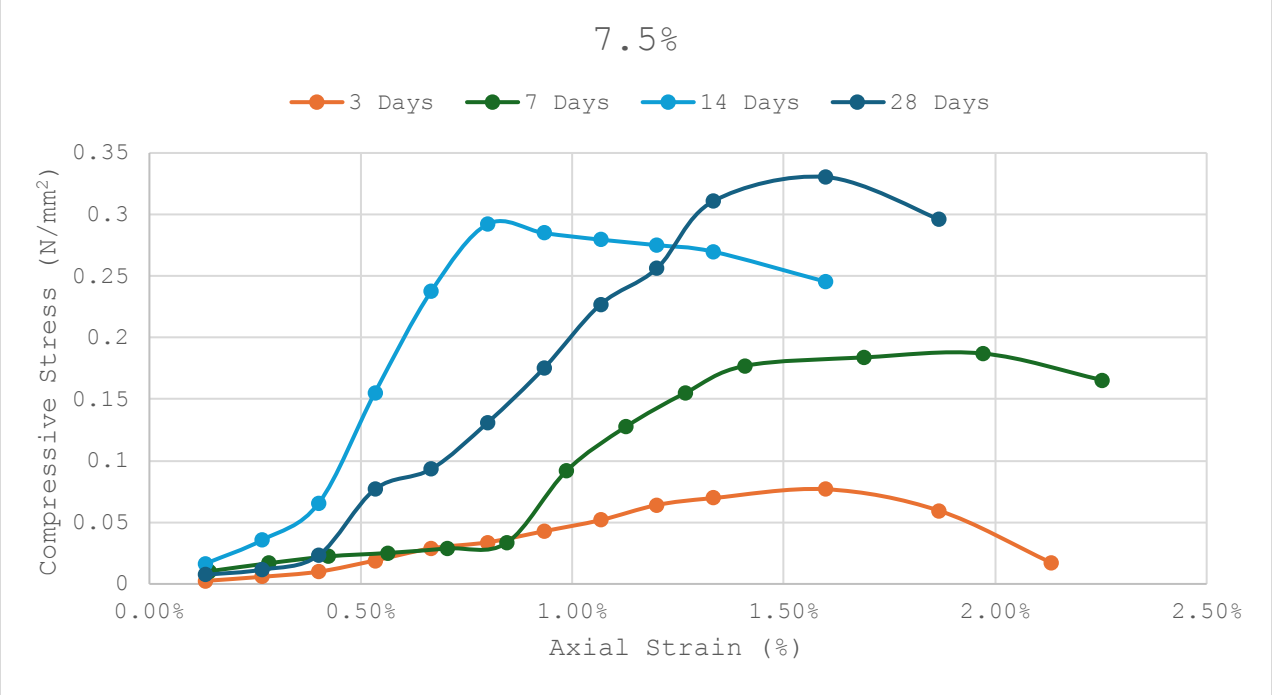

Figure 4-1 Graph showing elastic behavior of 7.5% mixture composition UCS test

Table 4-5 Peak UCS values of 7.5% mixture composition

Curing Period	Peak UCS value (kPa)
3 days	76.8819
7 days	187.0942
14 days	292.21772
28 days	330.42858

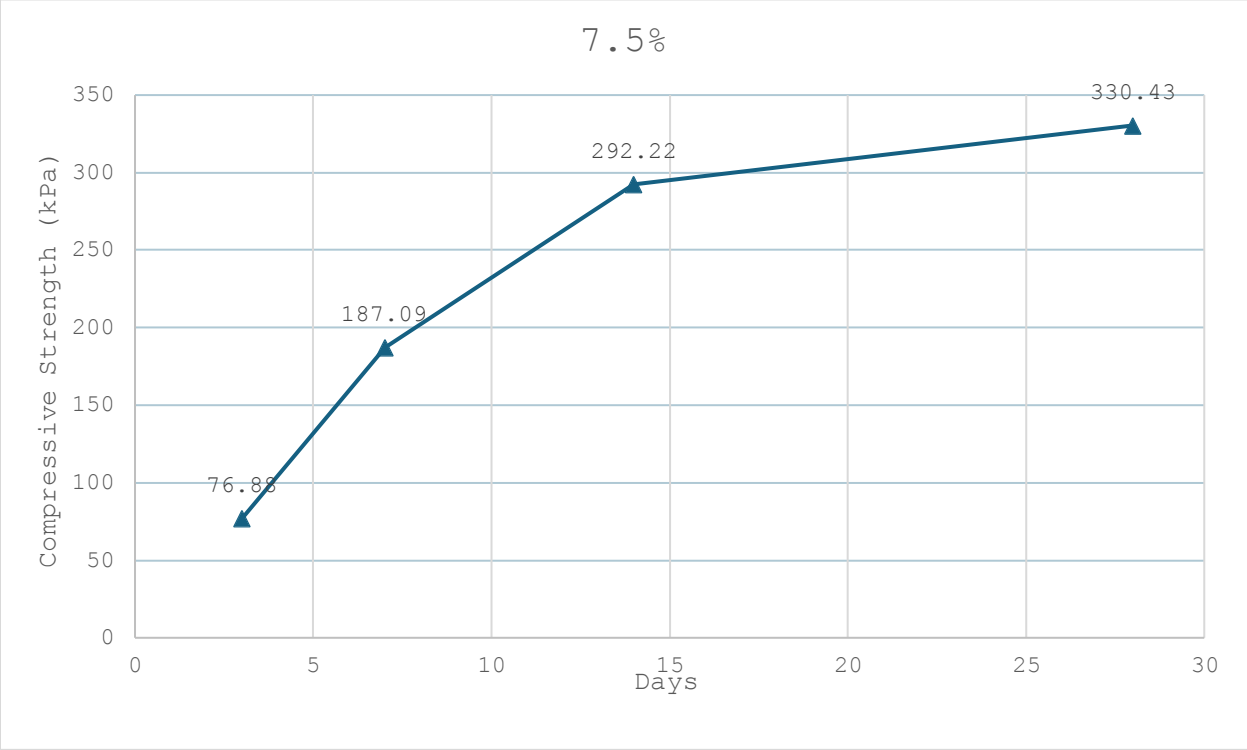

Figure 4-2 Graph showing trendline of peak UCS values of 7.5% mixture composition over curing periods

4.1.2 10% Mixture Composition

The diameter of the trimmed sample is 36.78 mm and the length of the sample is 76 mm for 3 days curing period.

Table 4-6 UCS test data of 3 days

load dial	calibrated (kg)	displacement dial gauge reading	unit strain L_0/L	corrected $A=A_0/(1-(L_0/L))$	stress Kg/mm^2	stress N/mm^2
1.1	1.11452	0.1	0.13%	1063.864123	0.001047615	0.010266627
2.3	2.33036	0.2	0.26%	1065.267637	0.002187582	0.021438301
5.1	5.16732	0.3	0.39%	1066.67486	0.004844325	0.047474388
6.8	6.88976	0.4	0.53%	1068.085806	0.006450568	0.063215565
9.6	9.72672	0.5	0.66%	1069.500489	0.009094638	0.089127454
13.1	13.27292	0.6	0.79%	1070.918924	0.012393954	0.12146075
15.4	15.60328	0.7	0.92%	1072.341128	0.014550668	0.142596549
16.8	17.02176	0.8	1.05%	1073.767113	0.015852376	0.155353285
18.1	18.33892	0.9	1.18%	1075.196896	0.017056336	0.167152097
19.8	20.06136	1	1.32%	1076.630492	0.018633468	0.182607988
20.72	20.993504	1.2	1.58%	1079.509183	0.019447268	0.190583223
18.3	18.54156	1.4	1.84%	1082.40331	0.017129992	0.167873921
12.6	12.76632	1.6	2.11%	1085.312996	0.0117628	0.115275443
3.1	3.14092	1.8	2.37%	1088.238368	0.002886243	0.028285178

The diameter of the trimmed sample is 39 mm and the length of the sample is 75 mm for 7 days curing period.

Table 4-7 UCS test data of 7 days

load dial	calibrated (kg)	displacement dial gauge reading	unit strain L_0/L	corrected $A=A_0/(1-(L_0/L))$	stress Kg/mm^2	stress N/mm^2
2.8	2.83696	0.1	0.13%	1196.188318	0.002371667	0.023242334
4.8	4.86336	0.2	0.27%	1197.7875	0.004060286	0.039790804
8.7	8.81484	0.3	0.40%	1199.390964	0.00734943	0.072024415
13.2	13.37424	0.4	0.53%	1200.998727	0.011135932	0.109132132
22.4	22.69568	0.5	0.67%	1202.610805	0.018872007	0.184945672
29.8	30.19336	0.6	0.80%	1204.227218	0.02507281	0.245713536
32.3	32.72636	0.7	0.93%	1205.847981	0.027139706	0.265969121
33.5	33.9422	0.8	1.07%	1207.473113	0.028110108	0.275479061
34.8	35.25936	0.9	1.20%	1209.102632	0.029161594	0.285783621
35.7	36.17124	1	1.33%	1210.736554	0.029875401	0.292778929
36	36.4752	1.2	1.60%	1214.017683	0.030045032	0.294441313
40	40.528	1.4	1.87%	1217.316644	0.033292899	0.32627041
44	44.5808	1.6	2.13%	1220.633583	0.036522672	0.357922186
40	40.528	1.8	2.40%	1223.968648	0.033111959	0.324497201
29	29.3828	2	2.67%	1227.321986	0.02394058	0.234617682

The diameter of the trimmed sample is 39 mm and the length of the sample is 75 mm for 14 days curing period.

Table 4-8 UCS test data of 14 days

load dial	calibrated (kg)	displacement dial gauge reading	unit strain L_0/L	corrected $A=A_0/(1-(L_0/L))$	stress Kg/mm^2	stress N/mm^2
1.3	1.31716	0.1	0.13%	1196.188318	0.001101131	0.010791083
2.3	2.33036	0.2	0.27%	1197.7875	0.001945554	0.019066427
2.6	2.63432	0.3	0.40%	1199.390964	0.002196381	0.021524538
2.7	2.73564	0.4	0.53%	1200.998727	0.002277804	0.022322482
3.3	3.34356	0.5	0.67%	1202.610805	0.002780251	0.027246461
4.2	4.25544	0.6	0.80%	1204.227218	0.003533752	0.034630767
6.5	6.5858	0.7	0.93%	1205.847981	0.005461551	0.053523198
9	9.1188	0.8	1.07%	1207.473113	0.007551969	0.0740093
12.5	12.665	0.9	1.20%	1209.102632	0.01047471	0.102652163
15.6	15.80592	1	1.33%	1210.736554	0.013054797	0.127937011
23.3	23.60756	1.2	1.60%	1214.017683	0.019445812	0.190568961
33.3	33.73956	1.4	1.87%	1217.316644	0.027716338	0.271620116
46.9	47.51908	1.6	2.13%	1220.633583	0.038929848	0.381512512
50.3	50.96396	1.8	2.40%	1223.968648	0.041638289	0.40805523
55.4	56.13128	2	2.67%	1227.321986	0.045734763	0.448200676
56.1	56.84052	2.2	2.93%	1230.69375	0.046185755	0.452620399
55.4	56.13128	2.4	3.20%	1234.084091	0.045484161	0.445744782
22.8	23.10096	2.6	3.47%	1237.493163	0.018667546	0.182941946

The diameter of the trimmed sample is 39 mm and the length of the sample is 75 mm for 28 days curing period.

Table 4-9 UCS test data of 28 days

load dial	calibrated (kg)	displacement dial gauge reading	unit strain L_0/L	corrected $A=A_0/(1-(L_0/L))$	stress Kg/mm^2	stress N/mm^2
1.1	1.11452	0.1	0.13%	1196.188318	0.000931726	0.009130917
1.4	1.41848	0.2	0.27%	1197.7875	0.00118425	0.011605651
2.4	2.43168	0.3	0.40%	1199.390964	0.002027429	0.019868804
5.1	5.16732	0.4	0.53%	1200.998727	0.004302519	0.042164688
5.8	5.87656	0.5	0.67%	1202.610805	0.004886502	0.047887719
7.3	7.39636	0.6	0.80%	1204.227218	0.006141997	0.060191571
8.9	9.01748	0.7	0.93%	1205.847981	0.007478123	0.073285609
13.7	13.88084	0.8	1.07%	1207.473113	0.011495776	0.112658601
22.4	22.69568	0.9	1.20%	1209.102632	0.018770681	0.183952675
31.3	31.71316	1	1.33%	1210.736554	0.026193279	0.256694131
48.3	48.93756	1.2	1.60%	1214.017683	0.040310418	0.395042094
58.9	59.67748	1.4	1.87%	1217.316644	0.049023794	0.480433178
53.3	54.00356	1.6	2.13%	1220.633583	0.044242237	0.43357392
41.8	42.35176	1.8	2.40%	1223.968648	0.034601997	0.339099575

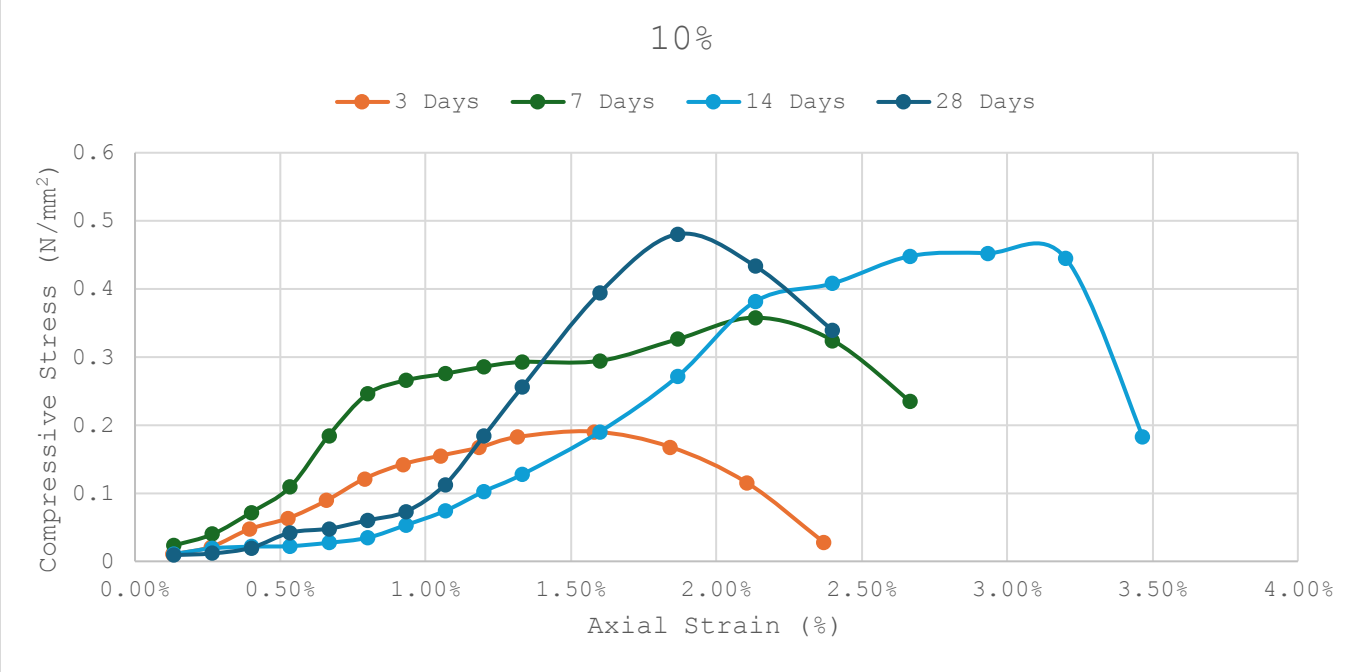

Figure 4-3 Graph showing elastic behavior of 10% mixture composition UCS test

Table 4-10 Peak UCS values of 10% mixture composition

Curing Period	Peak UCS value (kPa)
3 days	190.583
7 days	357.922
14 days	452.62
28 days	480.433

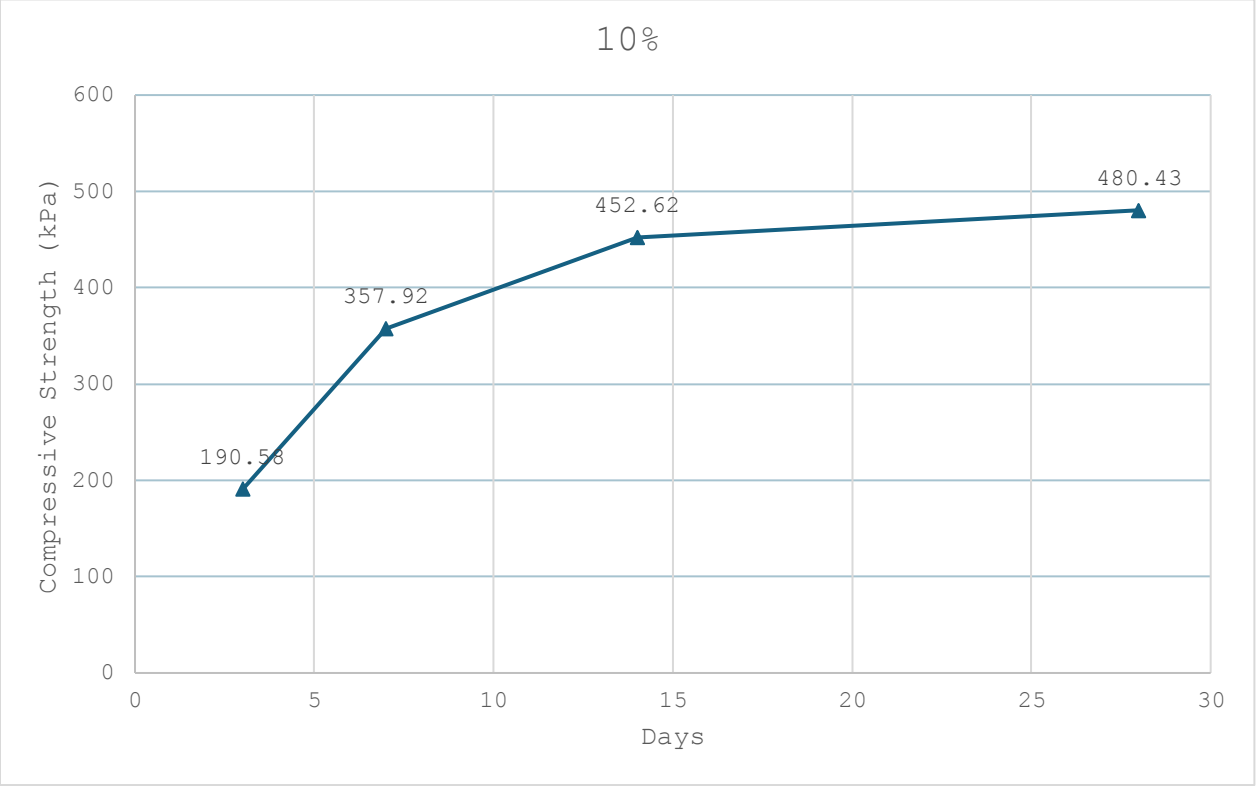

Figure 4-4 Graph showing trendline of peak UCS values of 10% mixture composition over curing periods

4.1.3 12.5% Mixture Composition

The diameter of the trimmed sample is 36.78 mm and the length of the sample is 76 mm for 3 days curing period.

Table 4-11 UCS test data of 3 days

load dial	calibrated (kg)	displacement dial gauge reading	unit strain L_0/L	corrected $A=A_0/(1-(L_0/L))$	stress Kg/mm^2	stress N/mm^2
1.3	1.31716	0.1	0.13%	1063.864123	0.00123809	0.012133286
3.2	3.24224	0.2	0.26%	1065.267637	0.003043592	0.029827201
7.3	7.39636	0.3	0.39%	1066.67486	0.006934034	0.067953536
8.6	8.71352	0.4	0.53%	1068.085806	0.008158071	0.079949097
10.9	11.04388	0.5	0.66%	1069.500489	0.010326204	0.101196797
17.7	17.93364	0.6	0.79%	1070.918924	0.01674603	0.16411109
23.4	23.70888	0.7	0.92%	1072.341128	0.022109457	0.216672678
27.9	28.26828	0.8	1.05%	1073.767113	0.026326267	0.257997419
34.1	34.55012	0.9	1.18%	1075.196896	0.032133761	0.314910857
41.5	42.0478	1	1.32%	1076.630492	0.039054996	0.382738965
42.65	43.21298	1.2	1.58%	1079.509183	0.040030211	0.392296064
36.1	36.57652	1.4	1.84%	1082.40331	0.033791951	0.331161123
21	21.2772	1.6	2.11%	1085.312996	0.019604667	0.192125738
4.2	4.25544	1.8	2.37%	1088.238368	0.003910393	0.038321854

The diameter of the trimmed sample is 38.61 mm and the length of the sample is 79.02 mm for 7 days curing period.

Table 4-12 UCS test data of 7 days

load dial	calibrated (kg)	displacement dial gauge reading	unit strain L_0/L	corrected $A=A_0/(1-(L_0/L))$	stress Kg/mm^2	stress N/mm^2
1.3	1.31716	0.1	0.13%	1172.304546	0.001123565	0.011010934
8.8	8.91616	0.2	0.25%	1173.791864	0.007596032	0.074441109
14	14.1848	0.3	0.38%	1175.282962	0.012069264	0.118278784
23	23.3036	0.4	0.51%	1176.777852	0.019802888	0.194068302
33	33.4356	0.5	0.63%	1178.27655	0.0283767	0.278091658
41.4	41.94648	0.6	0.76%	1179.779071	0.035554521	0.348434308
48	48.6336	0.7	0.89%	1181.285428	0.041170067	0.403466655
54	54.7128	0.8	1.01%	1182.795637	0.046257188	0.453320441
59	59.7788	0.9	1.14%	1184.309712	0.050475648	0.494661349
63.5	64.3382	1	1.27%	1185.827669	0.054255944	0.531708254
64	64.8448	1.2	1.52%	1188.875286	0.054542979	0.534521196
57	57.7524	1.4	1.77%	1191.938608	0.048452495	0.474834456
21.7	21.98644	1.6	2.02%	1195.017757	0.018398421	0.180304527

The diameter of the trimmed sample is 39 mm and the length of the sample is 75 mm for 14 days curing period.

Table 4-13 UCS test data of 14 days

load dial	calibrated (kg)	displacement dial gauge reading	unit strain L_0/L	corrected $A=A_0/(1-(L_0/L))$	stress Kg/mm^2	stress N/mm^2
1.6	1.62112	0.1	0.13%	1196.188318	0.00135524	0.013281334
3.2	3.24224	0.2	0.27%	1197.7875	0.00270686	0.026527203
4.7	4.76204	0.3	0.40%	1199.390964	0.00397038	0.038909741
6.8	6.88976	0.4	0.53%	1200.998727	0.00573669	0.056219583
12	12.1584	0.5	0.67%	1202.610805	0.01011	0.099078039
23.7	24.01284	0.6	0.80%	1204.227218	0.01994046	0.19541647
32.4	32.82768	0.7	0.93%	1205.847981	0.02722373	0.266792555
42.3	42.85836	0.8	1.07%	1207.473113	0.03549426	0.34784371
53.7	54.40884	0.9	1.20%	1209.102632	0.04499936	0.440993691
61.2	62.00784	1	1.33%	1210.736554	0.05121497	0.501906736
66.6	67.47912	1.2	1.60%	1214.017683	0.05558331	0.544716428
58.2	58.96824	1.4	1.87%	1217.316644	0.04844117	0.474723446
52.6	53.29432	1.6	2.13%	1220.633583	0.04366119	0.427879704
32.3	32.72636	1.8	2.40%	1223.968648	0.02673791	0.26203149

The diameter of the trimmed sample is 39 mm and the length of the sample is 75 mm for 28 days curing period.

Table 4-14 UCS test data of 28 days

load dial	calibrated (kg)	displacement dial gauge reading	unit strain L_0/L	corrected $A=A_0/(1-(L_0/L))$	stress Kg/mm^2	stress N/mm^2
2.5	2.533	0.1	0.13%	1196.188318	0.00211756	0.020752084
2.6	2.63432	0.2	0.27%	1197.7875	0.002199322	0.021553352
6.6	6.68712	0.3	0.40%	1199.390964	0.00557543	0.054639211
10.5	10.6386	0.4	0.53%	1200.998727	0.008858128	0.086809651
17	17.2244	0.5	0.67%	1202.610805	0.014322506	0.140360555
23	23.3036	0.6	0.80%	1204.227218	0.019351498	0.189644676
30.9	31.30788	0.7	0.93%	1205.847981	0.025963372	0.254441048
38.5	39.0082	0.8	1.07%	1207.473113	0.032305647	0.316595339
46	46.6072	0.9	1.20%	1209.102632	0.038546935	0.377759959
53	53.6996	1	1.33%	1210.736554	0.044352836	0.434657794
66.8	67.68176	1.2	1.60%	1214.017683	0.055750226	0.546352213
69.3	70.21476	1.4	1.87%	1217.316644	0.057679947	0.565263485
60.3	61.09596	1.6	2.13%	1220.633583	0.050052662	0.490516086

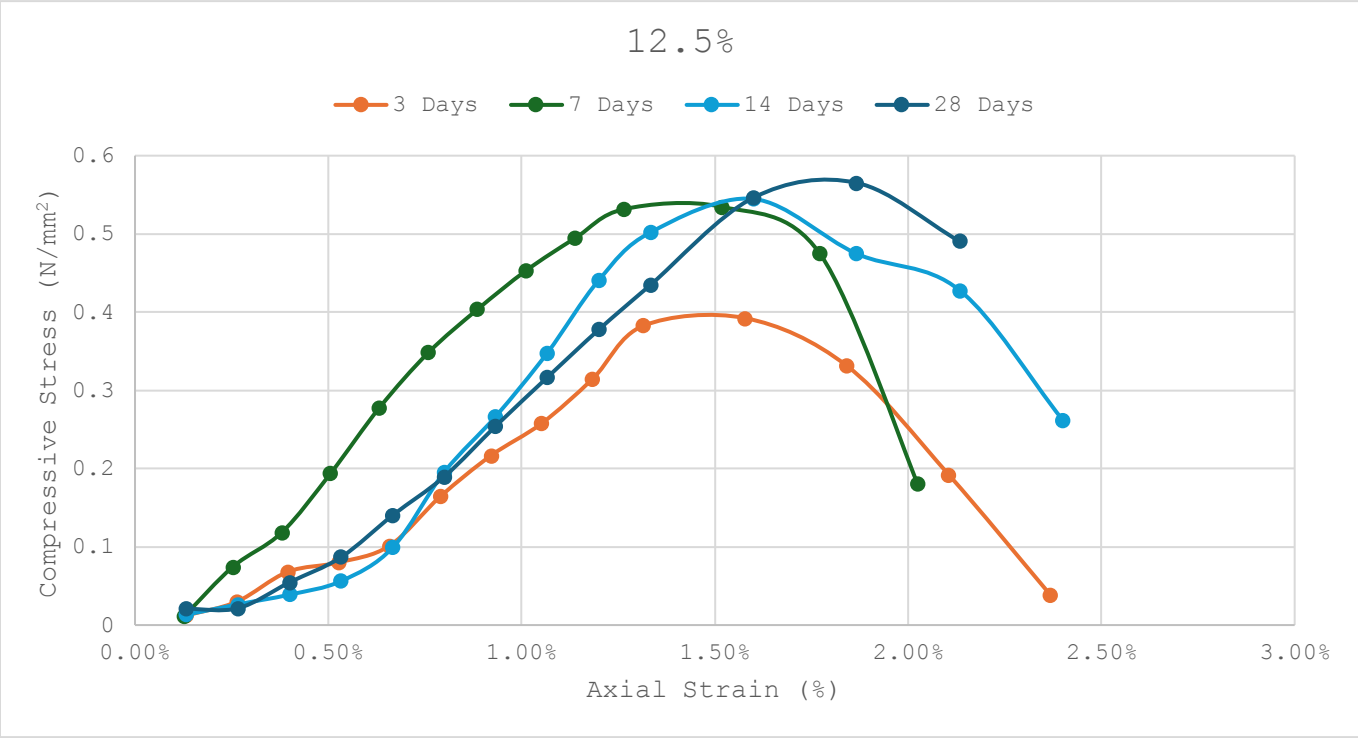

Figure 4-5 Graph showing elastic behavior of 12.5% mixture composition UCS test

Table 4-15 Peak UCS values of 12.5% mixture composition

Curing Period	Peak UCS value (kPa)
3 days	392.296
7 days	534.521
14 days	544.716
28 days	565.2635

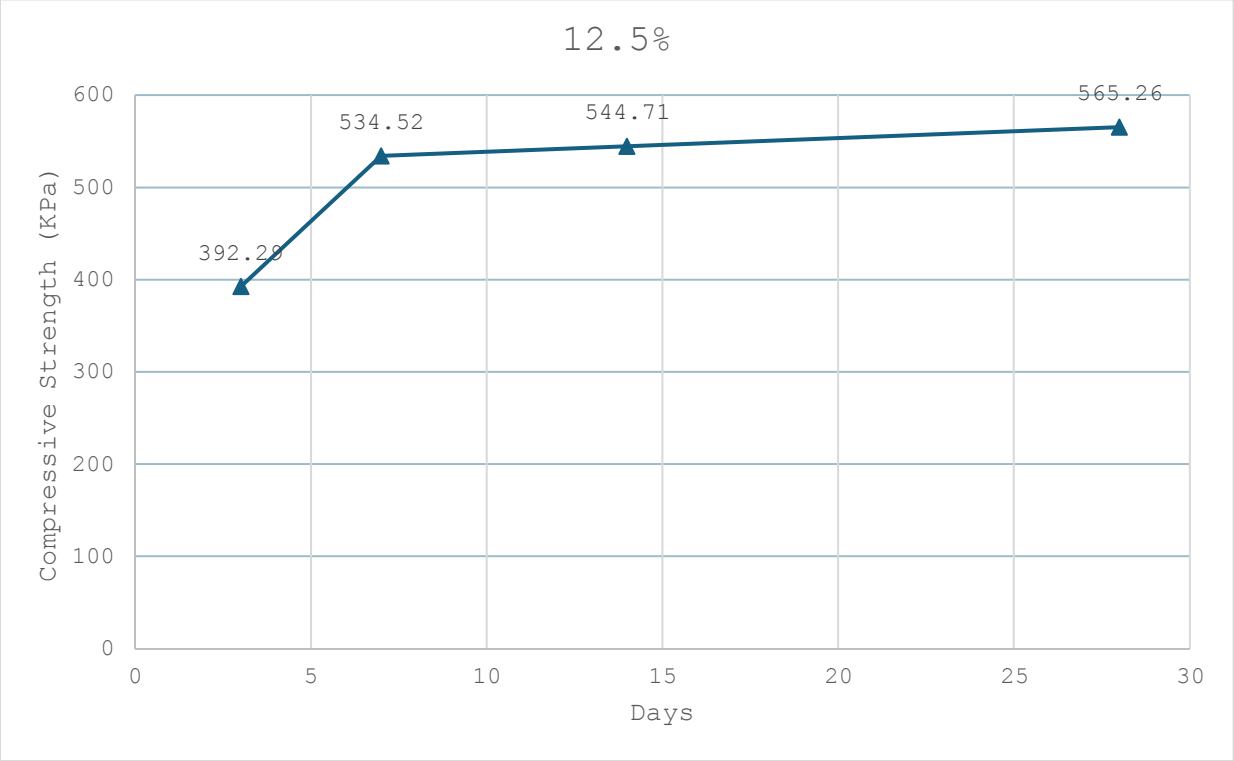

Figure 4-6 Graph showing trendline of peak UCS values of 12.5% mixture composition over curing periods

4.1.4 15% Mixture Composition

The diameter of the trimmed sample is 39 mm and the length of the sample is 75 mm for 3 days curing period.

Table 4-16 UCS test data of 3 days

Load dial	calibrated (kg)	displacement dial gauge reading	unit strain L_0/L	corrected $A=A_0/(1-(L_0/L))$	stress Kg/mm^2	stress N/mm^2
1.2	1.21584	0.1	0.13%	1196.188318	0.001016429	0.009961
4.3	4.35676	0.2	0.27%	1197.7875	0.00363734	0.035645929
8.6	8.71352	0.3	0.40%	1199.390964	0.007264954	0.071196548
11	11.1452	0.4	0.53%	1200.998727	0.009279943	0.090943444
14.3	14.48876	0.5	0.67%	1202.610805	0.012047755	0.118067996
15.6	15.80592	0.6	0.80%	1204.227218	0.013125364	0.128628563
18.2	18.44024	0.7	0.93%	1205.847981	0.015292342	0.149864954
23.1	23.40492	0.8	1.07%	1207.473113	0.019383388	0.189957204
29.3	29.68676	0.9	1.20%	1209.102632	0.024552721	0.240616669
38.4	38.90688	1	1.33%	1210.736554	0.032134885	0.314921874
46.3	46.91116	1.2	1.60%	1214.017683	0.038641249	0.378684244
53.1	53.80092	1.4	1.87%	1217.316644	0.044196323	0.433123969
45	45.594	1.6	2.13%	1220.633583	0.037352733	0.366056781
21.3	21.58116	1.8	2.40%	1223.968648	0.017632118	0.172794759

The diameter of the trimmed sample is 39 mm and the length of the sample is 75 mm for 7 days curing period.

Table 4-17 UCS test data of 7 days

load dial	calibrated (kg)	displacement dial gauge reading	unit strain L_0/L	corrected $A=A_0/(1-(L_0/L))$	stress Kg/mm^2	stress N/mm^2
1.4	1.41848	0.1	0.13%	1196.188318	0.001185833	0.011621167
6.3	6.38316	0.2	0.27%	1197.7875	0.005329126	0.052225431
8.3	8.40956	0.3	0.40%	1199.390964	0.007011525	0.068712947
10.7	10.84124	0.4	0.53%	1200.998727	0.009026854	0.088463168
14	14.1848	0.5	0.67%	1202.610805	0.011795005	0.115591045
20.3	20.56796	0.6	0.80%	1204.227218	0.0170798	0.16738204
29.5	29.8894	0.7	0.93%	1205.847981	0.024787038	0.242912975
38.3	38.80556	0.8	1.07%	1207.473113	0.032137825	0.314950688
46.1	46.70852	0.9	1.20%	1209.102632	0.038630732	0.378581176
54.6	55.32072	1	1.33%	1210.736554	0.04569179	0.447779539
61.3	62.10916	1.2	1.60%	1214.017683	0.051160013	0.501368124
67.7	68.59364	1.4	1.87%	1217.316644	0.056348231	0.552212668
60.2	60.99464	1.6	2.13%	1220.633583	0.049969656	0.489702627
24	24.3168	1.8	2.40%	1223.968648	0.019867176	0.19469832

The diameter of the trimmed sample is 38 mm and the length of the sample is 80 mm for 14 days curing period.

Table 4-18 UCS test data of 14 days

load dial	calibrated (kg)	displacement dial gauge reading	unit strain L_0/L	corrected $A=A_0/(1-(L_0/L))$	stress Kg/mm^2	stress N/mm^2
2.1	2.12772	0.1	0.13%	1135.537021	0.001873757	0.018362815
6.5	6.5858	0.2	0.25%	1136.96	0.005792464	0.056766148
19.5	19.7574	0.3	0.38%	1138.38655	0.017355616	0.170085038
41	41.5412	0.4	0.50%	1139.816683	0.03644551	0.357165995
61.5	62.3118	0.5	0.63%	1141.250415	0.054599586	0.535075941
72.9	73.86228	0.6	0.75%	1142.687758	0.064639075	0.633462938
80	81.056	0.7	0.88%	1144.128726	0.070845175	0.694282716
70	70.924	0.8	1.00%	1145.573333	0.061911357	0.606731302
65	65.858	1	1.25%	1148.473519	0.057343943	0.561970641
41	41.5412	1.2	1.50%	1151.388426	0.036079223	0.353576387

The diameter of the trimmed sample is 39 mm and the length of the sample is 75 mm for 28 days curing period.

Table 4-19 UCS test data of 28 days

load dial	calibrated (kg)	displacement dial gauge reading	unit strain L_0/L	corrected $A=A_0/(1-(L_0/L))$	stress Kg/mm^2	stress N/mm^2
1.8	1.82376	0.1	0.13%	1196.188318	0.001524643	0.0149415
2.2	2.22904	0.2	0.27%	1197.7875	0.001860964	0.018237452
6.3	6.38316	0.3	0.40%	1199.390964	0.005322001	0.052155611
13.3	13.47556	0.4	0.53%	1200.998727	0.011220295	0.109958891
25	25.33	0.5	0.67%	1202.610805	0.021062508	0.206412581
33	33.4356	0.6	0.80%	1204.227218	0.027765192	0.272098882
41	41.5412	0.7	0.93%	1205.847981	0.034449782	0.337607863
46	46.6072	0.8	1.07%	1207.473113	0.038598955	0.378269756
50	50.66	0.9	1.20%	1209.102632	0.041898842	0.410608651
62	62.8184	1	1.33%	1210.736554	0.05188445	0.508467608
93.9	95.13948	1.2	1.60%	1214.017683	0.078367458	0.76800109
101.2	102.53584	1.4	1.87%	1217.316644	0.084231034	0.825464136
69	69.9108	1.6	2.13%	1220.633583	0.05727419	0.561287064

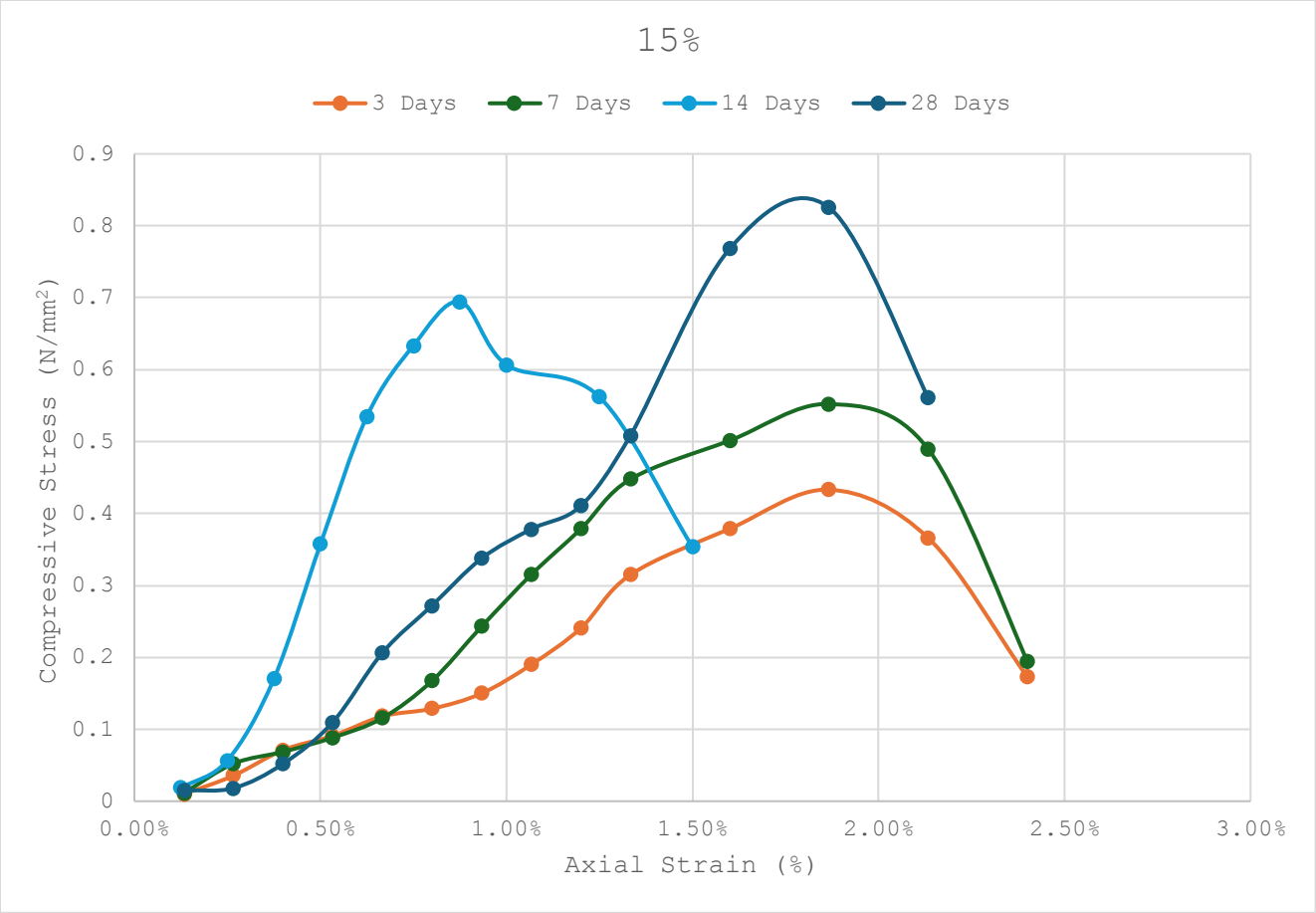

Figure 4-7 Graph showing elastic behavior of 15% mixture composition UCS test

Table 4-20 Peak UCS values of 15% mixture composition

Curing Period	Peak UCS value (kPa)
3 days	433.124
7 days	552.21
14 days	694.2827
28 days	825.46

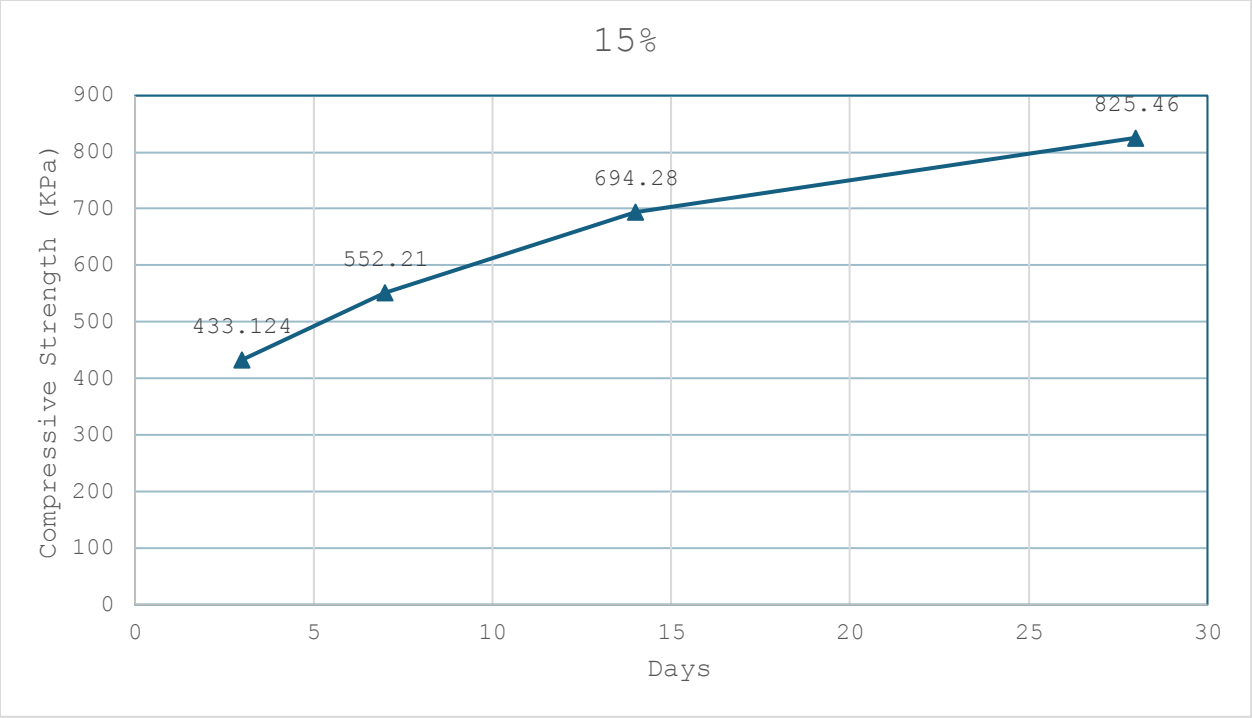

Figure 4-8 Graph showing trendline of peak UCS values of 15% mixture composition over curing periods

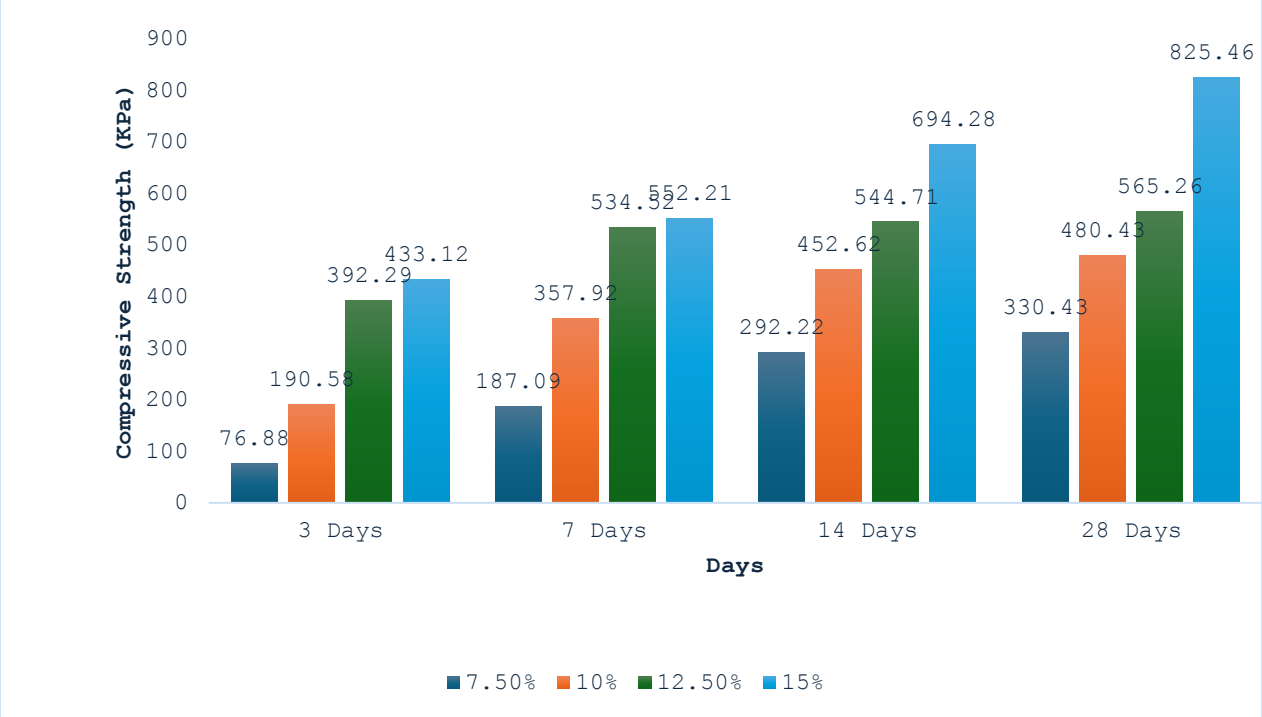

Figure 4-9 Graph showing trendline of peak UCS values of mixture compositions over curing periods

4.2 California Bearing Ratio Test (Unsoaked)

The Calibration factor of the California Bearing Ratio test is 0.0422D. The height of the disc and the mold is 2.416 inch and 7 inches respectively.

4.2.1 7.5% Mixture Composition

Table 4-21 CBR test data of 3 days

Penetration Reading	Penetration (mm)	Proving Ring Dial	Load (kN)
50	0.635	63	2.6586
100	1.27	125	5.275
150	1.905	169	7.1318
200	2.54	211	8.9042
250	3.175	259	10.9298
300	3.81	243	10.2546
350	4.445	199	8.3978
400	5.08	107	4.5154

Table 4-22 CBR test data of 7 days

Penetration Reading	Penetration (mm)	Proving Ring Dial	Load (kN)
50	0.635	85	3.587
100	1.27	147	6.2034
150	1.905	201	8.4822
200	2.54	266	11.2252
250	3.175	299	12.6178
300	3.81	334	14.0948
350	4.445	361	15.2342
400	5.08	389	16.4158

Table 4-23 CBR test data of 14 days

Penetration Reading	Penetration (mm)	Proving Ring Dial	Load (kN)
50	0.635	123	5.1906
100	1.27	208	8.7776
150	1.905	283	11.9426
200	2.54	373	15.7406
250	3.175	441	18.6102
300	3.81	483	20.3826
350	4.445	539	22.7458
400	5.08	585	24.687

Table 4-24 CBR test data of 28 days

Penretration Reading	Penetration (mm)	Proving Ring Dial	Load (kN)
50	0.635	135	5.697
100	1.27	253	10.6766
150	1.905	342	14.4324
200	2.54	451	19.0322
250	3.175	526	22.1972
300	3.81	595	25.109
350	4.445	646	27.2612
400	5.08	691	29.1602

Table 4-25 CBR values (2.54 mm & 5.08 mm) of 7.5% mixture composition

Curing Period	**CBR values (%)**
3 days	66
7 days	83
14 days	123
28 days	145

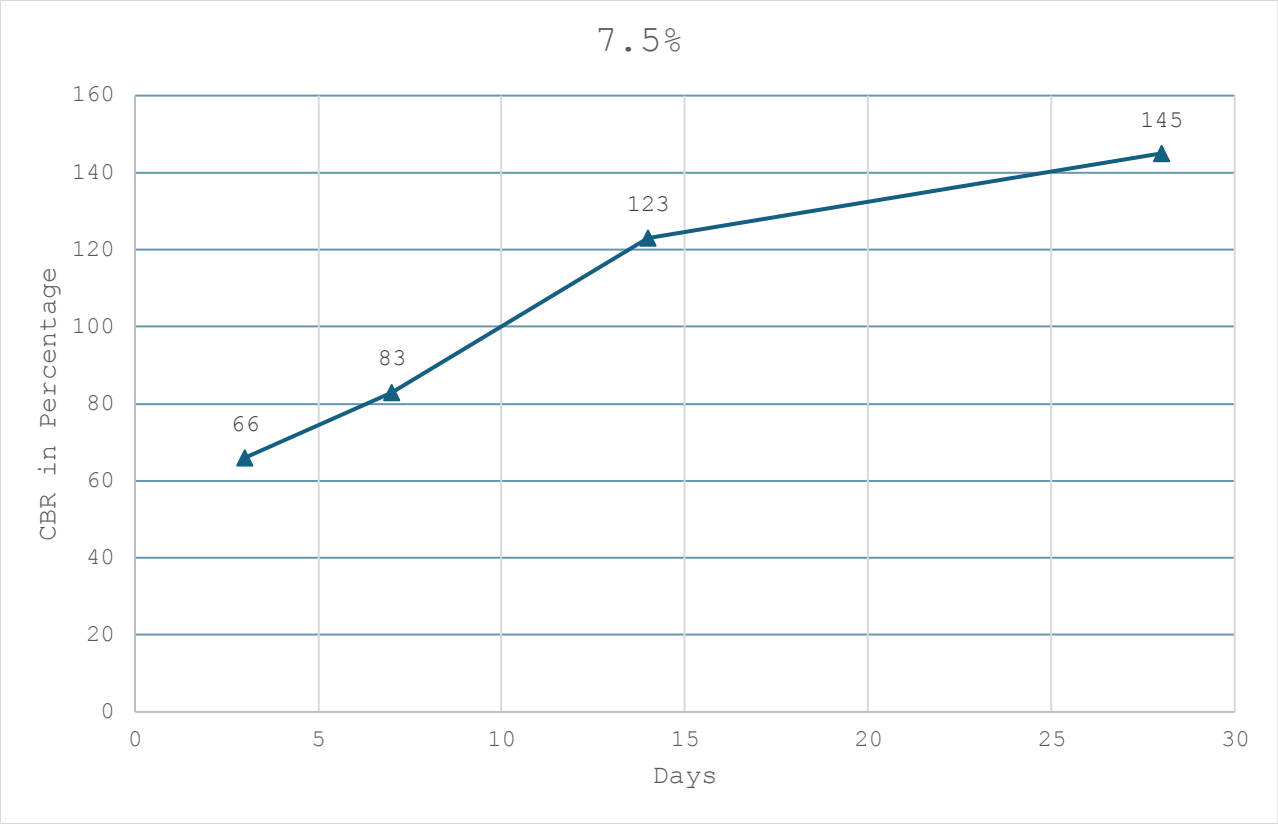

Figure 4-10 Graph showing trendline of CBR values of 7.5% mixture compositions over curing periods

4.2.2 10% Mixture Composition

Table 4-26 CBR test data of 3 days

Penetration Reading	Penetration (mm)	Proving Ring Dial	Load (kN)
50	0.635	73	3.0806
100	1.27	145	6.119
150	1.905	208	8.7776
200	2.54	262	11.0564
250	3.175	308	12.9976
300	3.81	310	13.082
350	4.445	300	12.66
400	5.08	276	11.6472

Table 4-27 CBR test data of 7 days

Penetration Reading	Penetration (mm)	Proving Ring Dial	Load (kN)
50	0.635	120	5.064
100	1.27	204	8.6088
150	1.905	267	11.2674
200	2.54	329	13.8838
250	3.175	375	15.825
300	3.81	421	17.7662
350	4.445	435	18.357
400	5.08	400	16.88

Table 4-28 CBR test data of 14 days

Penetration Reading	Penetration (mm)	Proving Ring Dial	Load (kN)
50	0.635	157	6.6254
100	1.27	249	10.5078
150	1.905	338	14.2636
200	2.54	408	17.2176
250	3.175	493	20.8046
300	3.81	543	22.9146
350	4.445	587	24.7714
400	5.08	619	26.1218

Table 4-29 CBR test data of 28 days

Penetration Reading	Penetration (mm)	Proving Ring Dial	Load (kN)
50	0.635	148	6.2456
100	1.27	293	12.3646
150	1.905	398	16.7956
200	2.54	490	20.678
250	3.175	570	24.054
300	3.81	648	27.3456
350	4.445	723	30.5106
400	5.08	793	33.4646

Table 4-30 CBR values (2.54 mm & 5.08 mm) of 10% mixture composition

Curing Period	CBR values (%)
3 days	82
7 days	103
14 days	130
28 days	167

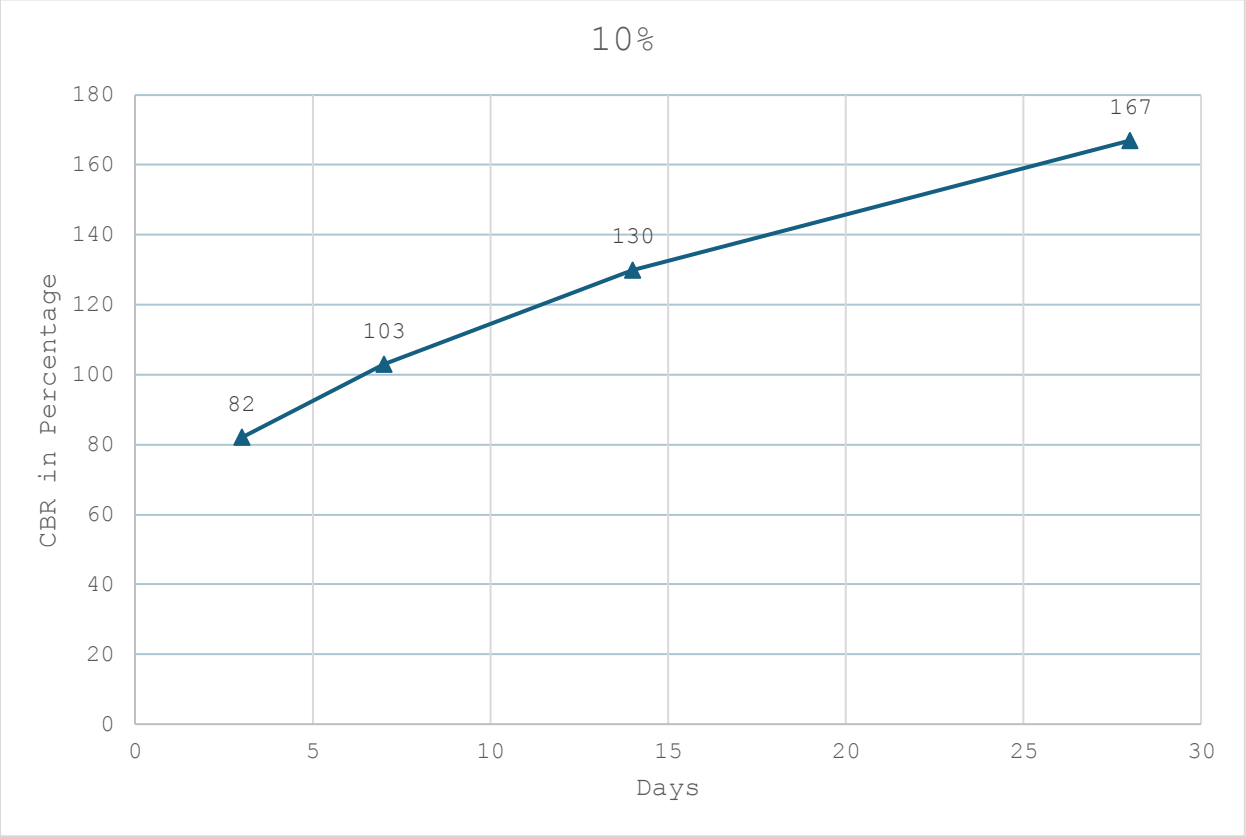

Figure 4-11 Graph showing trendline of CBR values of 10% mixture compositions over curing periods

4.2.3 12.5% Mixture Composition

Table 4-31 CBR test data of 3 days

Penetration Reading	Penetration (mm)	Proving Ring Dial	Load (kN)
50	0.635	106	4.4732
100	1.27	251	10.5922
150	1.905	356	15.0232
200	2.54	448	18.9056
250	3.175	528	22.2816
300	3.81	606	25.5732
350	4.445	630	28.7382
400	5.08	649	30.806

Table 4-32 CBR test data of 7 days

Penetration Reading	Penetration (mm)	Proving Ring Dial	Load (kN)
50	0.635	200	8.44
100	1.27	358	15.1076
150	1.905	468	19.7496
200	2.54	557	23.5054
250	3.175	603	25.4466
300	3.81	652	25.7842
350	4.445	681	25.953
400	5.08	730	26.164

Table 4-33 CBR test data of 14 days

Penetration Reading	Penetration (mm)	Proving Ring Dial	Load (kN)
50	0.635	245	10.339
100	1.27	390	16.458
150	1.905	495	20.889
200	2.54	587	24.7714
250	3.175	667	28.1474
300	3.81	745	31.439
350	4.445	820	34.604
400	5.08	890	37.558

Table 4-34 CBR test data of 28 days

Penetration Reading	Penetration (mm)	Proving Ring Dial	Load (kN)
50	0.635	430	18.146
100	1.27	608	25.6576
150	1.905	735	31.017
200	2.54	835	35.237
250	3.175	915	38.613
300	3.81	955	40.301
350	4.445	1005	42.411
400	5.08	1050	44.31

Table 4-35 CBR values (2.54 mm & 5.08 mm) of 12.5% mixture composition

Curing Period	**CBR values (%)**
3 days	141
7 days	175
14 days	187
28 days	262

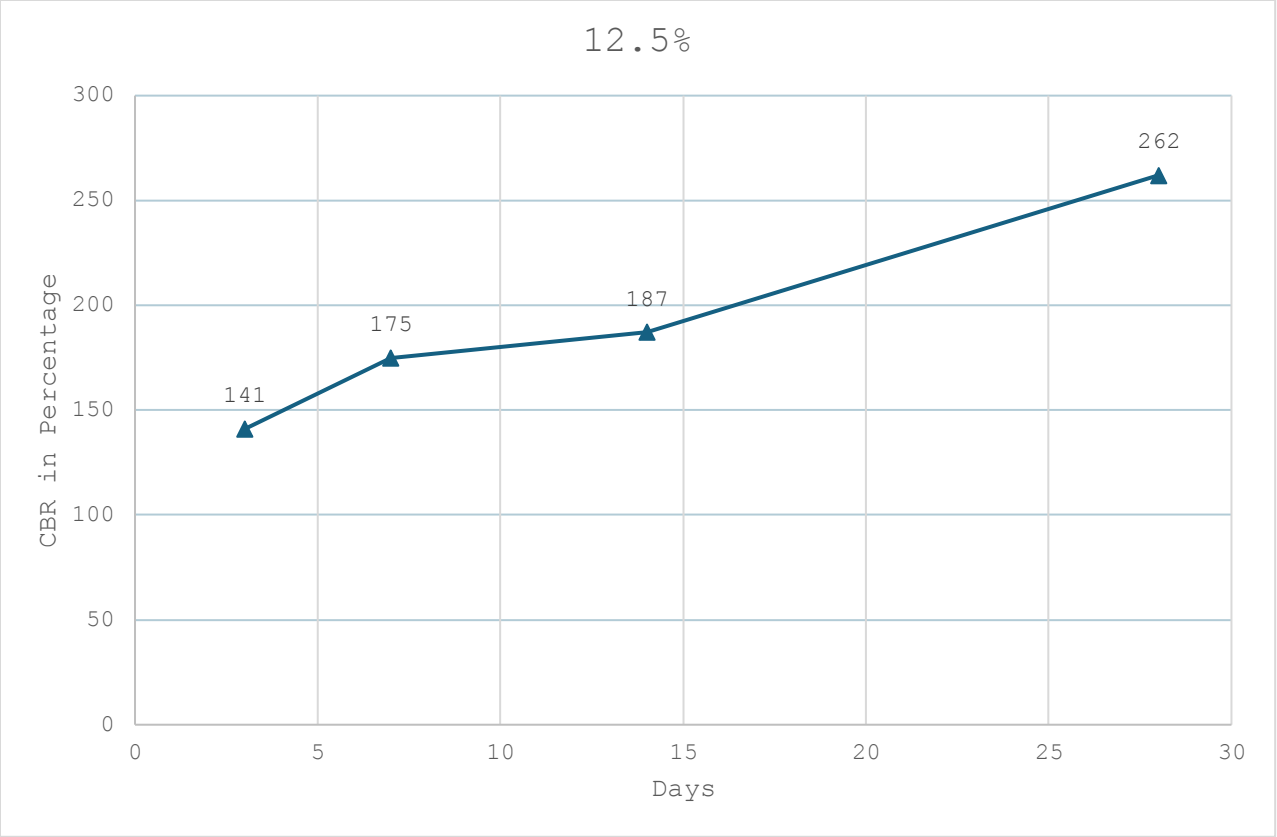

Figure 4-12 Graph showing trendline of CBR values of 12.5% mixture compositions over curing periods

4.2.4 15% Mixture Composition

Table 4-36 CBR test data of 3 days

Penetration Reading	Penetration (mm)	Proving Ring Dial	Load (kN)
50	0.635	170	7.174
100	1.27	315	13.293
150	1.905	420	17.724
200	2.54	512	21.6064
250	3.175	592	24.9824
300	3.81	670	28.274
350	4.445	745	31.439
400	5.08	815	34.393

Table 4-37 CBR test data of 7 days

Penetration Reading	Penetration (mm)	Proving Ring Dial	Load (kN)
50	0.635	203	8.5666
100	1.27	368	15.5296
150	1.905	501	21.1422
200	2.54	607	25.6154
250	3.175	685	28.907
300	3.81	776	32.7472
350	4.445	856	36.1232
400	5.08	936	39.4992

Table 4-38 CBR test data of 14 days

Penetration Reading	Penetration (mm)	Proving Ring Dial	Load (kN)
50	0.635	208	8.7776
100	1.27	458	19.3276
150	1.905	624	26.3328
200	2.54	730	30.806
250	3.175	821	34.6462
300	3.81	905	38.191
350	4.445	985	41.567
400	5.08	1075	45.365

Table 4-39 CBR test data of 28 days

Penetration Reading	Penetration (mm)	Proving Ring Dial	Load (kN)
50	0.635	343	14.4746
100	1.27	615	25.953
150	1.905	775	32.705
200	2.54	885	37.347
250	3.175	975	41.145
300	3.81	1055	44.521
350	4.445	1110	46.842
400	5.08	1155	48.741

Table 4-40 CBR values (2.54 mm & 5.08 mm) of 15% mixture composition

Curing Period	**CBR values (%)**
3 days	171
7 days	197
14 days	229
28 days	278

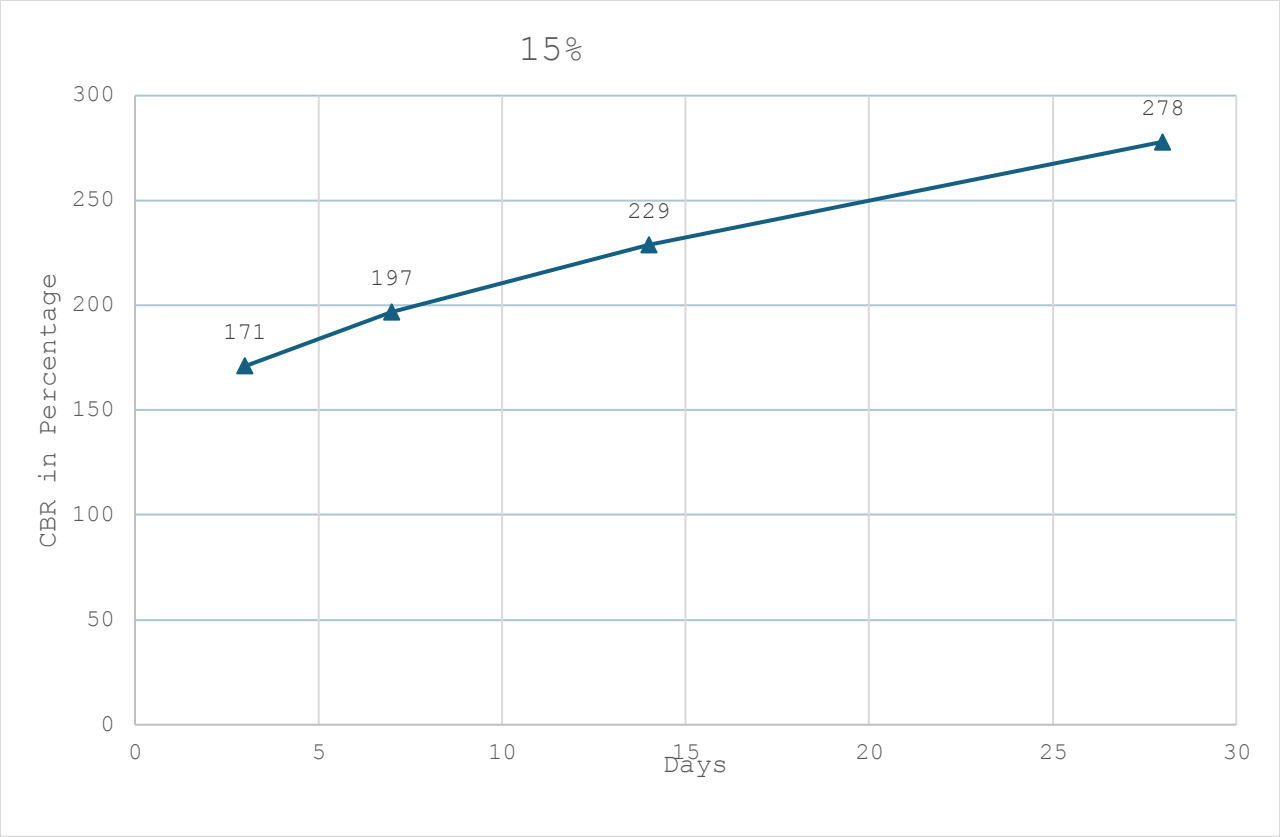

Figure 4-13 Graph showing trendline of CBR values of 15% mixture compositions over curing periods

4.2.5 Behavior of Loads (kN) under Settlement (mm)

Table 4-41 CBR Load (kN) Values for 3 Days

Settlement (mm)	7.5%	10%	12.5%	15%
0.635	2.6586	3.0806	4.4732	7.174
1.27	5.275	6.119	10.5922	13.293
1.905	7.1318	8.7776	15.0232	17.724
2.54	8.9042	11.0564	18.9056	21.6064
3.175	10.9298	12.9976	22.2816	24.9824
3.81	10.2546	13.082	25.5732	28.274
4.445	8.3978	12.66	26.586	31.439
5.08	4.5154	11.6472	27.3878	34.393

Table 4-42 CBR Load (kN) Values for 7 Days

Settlement (mm)	7.5%	10%	12.5%	15%
0.635	3.587	5.064	8.44	8.5666
1.27	6.2034	8.6088	15.1076	15.5296
1.905	8.4822	11.2674	19.7496	21.1422
2.54	11.2252	13.8838	23.5054	25.6154
3.175	12.6178	15.825	25.4466	28.907
3.81	14.0948	17.7662	27.5144	32.7472
4.445	15.2342	18.357	28.7382	36.1232
5.08	16.4158	16.88	30.806	39.4992

Table 4-43 CBR Load (kN) Values for 14 Days

Settlement (mm)	7.5%	10%	12.5%	15%
0.635	5.1906	6.6254	10.339	8.7776
1.27	8.7776	10.5078	16.458	19.3276
1.905	11.9426	14.2636	20.889	26.3328
2.54	15.7406	17.2176	24.7714	30.806
3.175	18.6102	20.8046	28.1474	34.6462
3.81	20.3826	22.9146	31.439	38.191
4.445	22.7458	24.7714	34.604	41.567
5.08	24.687	26.1218	37.558	45.365

Table 4-44 CBR Load (kN) Values for 28 Days

Settlement (mm)	7.5%	10%	12.5%	15%
0.635	5.697	6.2456	18.146	14.4746
1.27	10.6766	12.3646	25.6576	25.953
1.905	14.4324	16.7956	31.017	32.705
2.54	19.0322	20.678	35.237	37.347
3.175	22.1972	24.054	38.613	41.145
3.81	25.109	27.3456	40.301	44.521
4.445	27.2612	30.5106	42.411	46.842
5.08	29.1602	33.4646	44.31	48.741

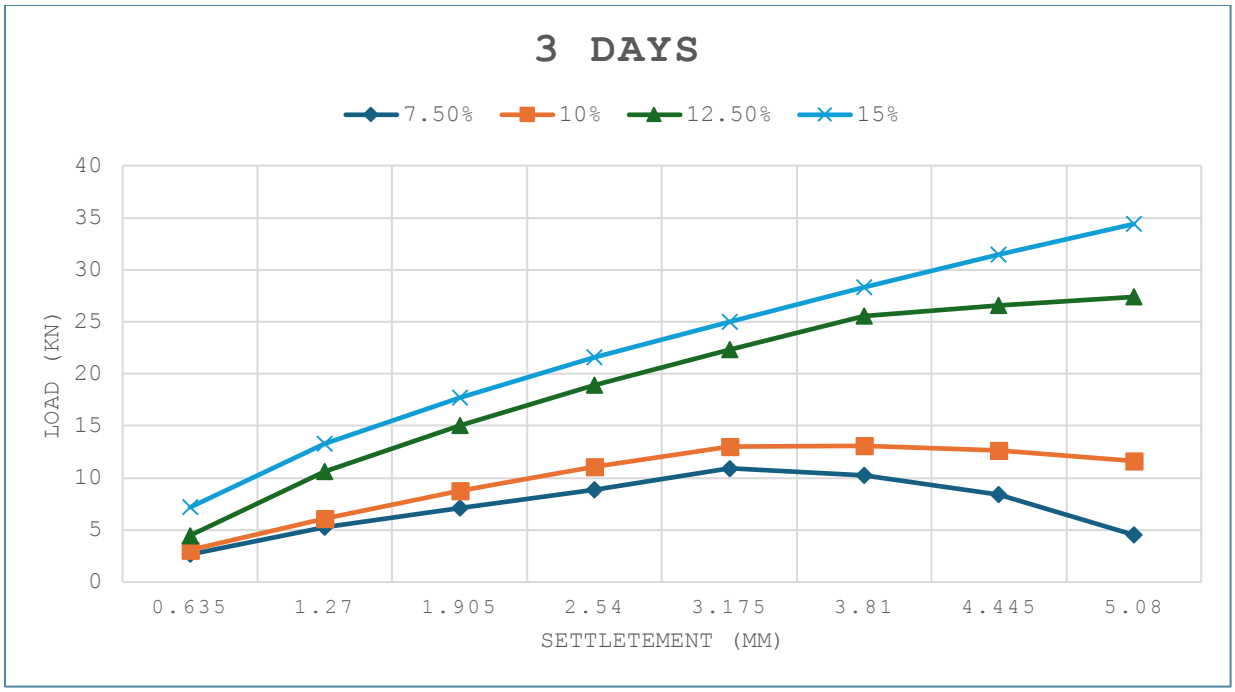

Figure 4-14 Graph showing trendline of loads (kN) over different settlements in 3 days curing period

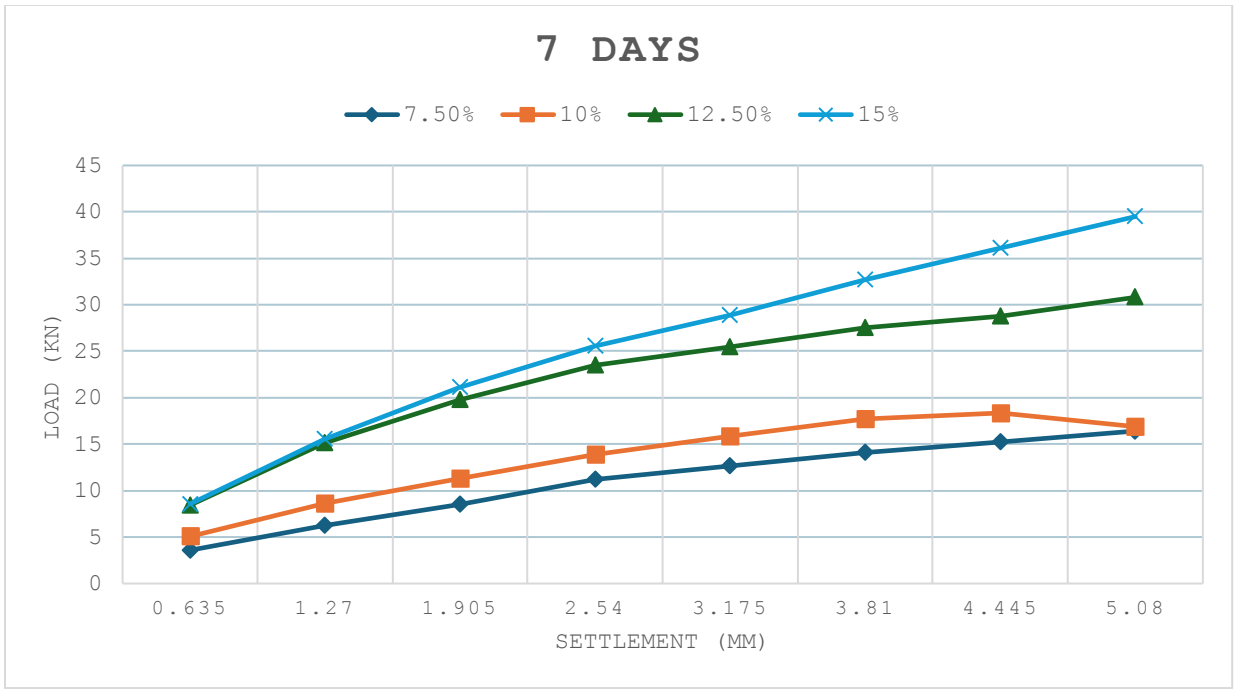

Figure 4-15 Graph showing trendline of loads (kN) over different settlements in 7 days curing period

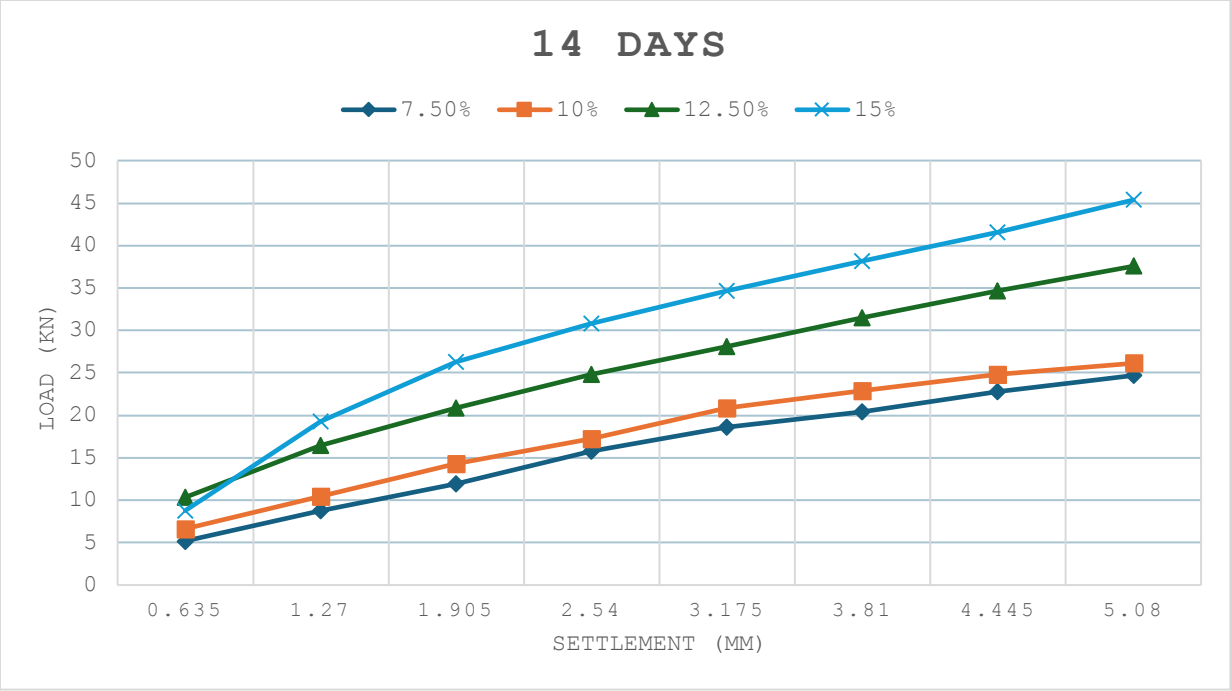

Figure 4-16 Graph showing trendline of loads (kN) over different settlements in 14 days curing period

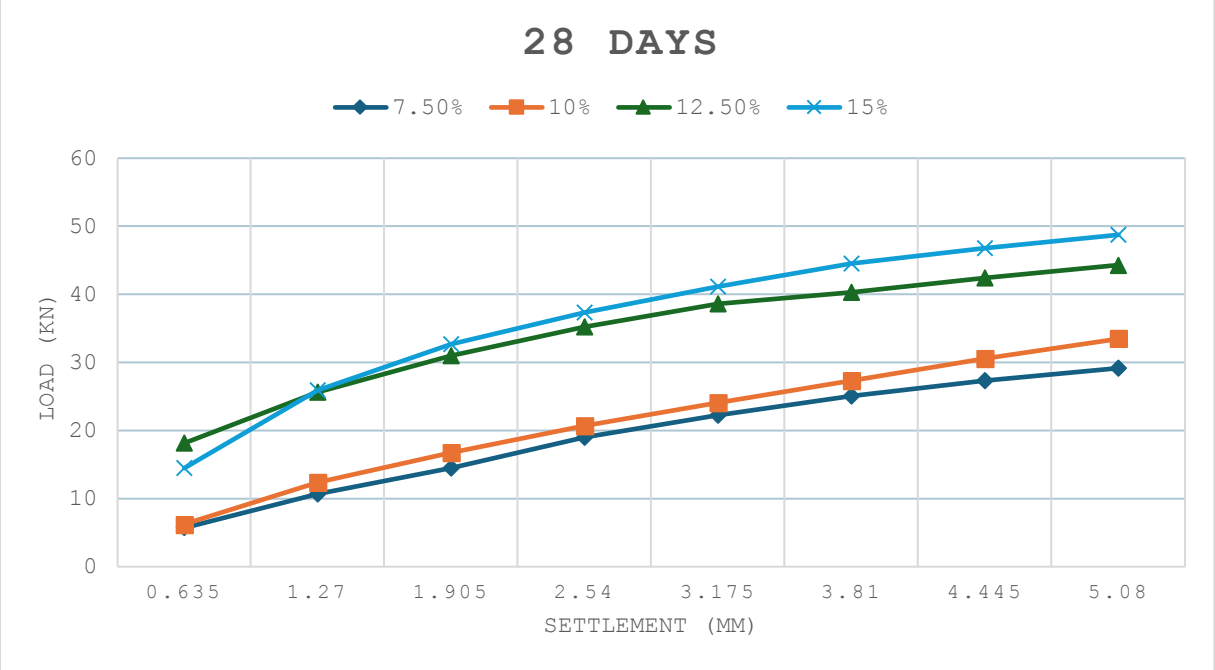

Figure 4-17 Graph showing trendline of loads (kN) over different settlements in 28 days curing period

4.3 Discussion

4.3.1 Unconfined Compressive Strength test

4.3.1.1 Graphical Interpretation of Compressive Stress Vs Axial Strain

The graphical interpretation of compressive stress vs axial strains over an increased curing periods of a particular SB-95 dosage results in the rising of the compressive stress of the soil. This behavior indicates that the compressive strength of the soil will increase over higher curing periods. On the other hand, the axial strain of the soil is noticed the lowest in the highest curing periods of a particular SB-95 dosage and vice versa. The decrement of axial strain over higher curing periods increases the density of the soil that indicates the soil stiffness and strength. The significant understanding of the graph is the minimal variation of the axial strain levels maintaining a constant duration while adjusting SB-95 dosages, whereas compressive stress consistently increases with higher SB-95 concentrations.

4.3.1.2 Graphical Interpretation of Compressive Stress Vs Days

The graph demonstrates a clear trend of increasing compressive strength as the duration progresses from 3 days to 28 days. The compressive strength of the material also increases with the percentage of SB-95 used. Higher SB-95 content enhances the material's mechanical properties, leading to improved compressive strength. The curves for 14 days and 28 days are nearly parallel to the X-axis, indicating that the change in compressive strength between these two time points is minimal. This suggests that the majority of strength development occurs within the first 14 days, with only slight additional gains between 14 and 28 days. A test conducted after 28 days showed that the change in compressive strength was not significant. This indicates that most of the strength is gained within the first 28 days, and further curing beyond this period does not substantially enhance compressive strength.

4.3.1.3 Crack Formation of UCS Molds

The mold samples of different proportions of the mixture after the UCS test explains the nature of the failure. We've managed to show a sample failure of each mixture proportion. There are various types of cracks observed in our mold samples. The crack formation of the mixture proportions of 7.5%, 10%, 12.5% and 15% SB-95 contents are depicted below.

Figure 4-18 7.5% Crack Formation

Figure 4-19 10% Crack Formation

Figure 4-20 12.5% Crack Formation

Figure 4-21 15% Crack Formation

The 7.5% sample crack exhibits a vertical crack with material failure at the top of the sample. This type of cracking leads to less ductility and lower strength by occurring a brittle collapse like cement and lime. (Hadi Fatehi 1, 2021) The crack suggests that the mixture of the binder and the chemical is not effective which leads to insufficient cohesion within the soil matrix.

The 10% sample has experienced a combination of shear and compressive forces that leads to failure along a plane of weakness because of the presence of the inclined shear cracks. The shear strength improvement occurs by creating an interlocking matrix among the bonds of the mixture of the binder and the chemical and the soil particles. (Sakina Tamassoki 1, 2022) The cracking of the sample suggests that the mixture of the binder and the chemical is sufficient to provide effective stabilization but not enough to prevent shear failure, having moderate strength and low ductility.

The observation on the 12.5% sample crack indicates a strong brittle failure because of the vertical cracks running along the length of the sample. This type of cracks having multiple planes of failure results in an effective stabilization with the mixture of binder and chemical, high compressive strength but low ductility as well as brittle stiffness. (Chibuzor2, 2022)

The sample of the 15% mixture exhibits a centralized vertical crack with minimum lateral spreading. The crack pattern suggests that the sample could handle more stress before failure as it is more controlled and centralized. The higher compaction of the soil develops stronger cohesion among the soil particles that leads to higher compressive strength. (Arif Ali Baig Moghal, 2017)The uniform and minimal cracking represents higher compressive strength and better cohesion between soil particles due to the binder. This kind of crack indicates that the sample has higher compressive strength and has less material loss with a cohesive crack pattern which is an indicator of improved soil strength due to effective stabilization. It should be noted that the distribution of the stabilizer contents is significant to their effectiveness in strengthening the soils. (Michael Z. Izzo 1 and Marta Mileti´ c 2, 2022)

4.3.1.4 Applicability of UCS Values of Stabilized Sandy Soil

The UCS value above 200 kPA recommends that the soil can support loads with acceptable levels of deformation. It refers to the ability of the soil undertaking moderate loads which is suitable for construction applications. (Joseph E. Bowles, 1996) Residential buildings, road subgrades are typically built using soil with supporting capacities in the range of 200-250 kPA. The maximum UCS value of our stabilized soil is 825.46 kPA which exceeds the typical range. According to the results of the UCS tests, the usage of high dosages of these stabilizers will be applicable in building high-rise structures, bridges and highways.

4.3.2 California Bearing Ratio test

4.3.2.1 Graphical Interpretation of Load Vs Settlement

The demonstration of the graph for any provided settlement value shows an upward trend of load in soil with the increment of SB-95 content. The increment is apparent across all tested percentage content of SB-95. The trend was observed consistently across different time intervals at 3 days, 7 days, 14 days and 28 days. Another observation of this graph indicates that the load in soil keeps increasing as the time progresses from 3 days to 28 days for a particular settlement value.

4.3.2.2 Graphical Interpretation of CBR in Percentage Vs Days

The graphical demonstration of the CBR in Percentage Vs Days shows a clear trend of the increment of the CBR values as the duration progresses from 3 days to 28 days. The effect of SB-95 content has a major contribution in increasing the CBR values because the higher CBR value of the soil is obtained with the higher mixture proportion of SB-95 content.

4.3.2.3 Applicability of CBR Values as a Subbase Material

The CBR value above 80% is defined as an excellent relative rating as a subbase material. The pavement gets more strength with the increment of CBR values. (Design Manual, 2013)The maximum average CBR values of our stabilized soil is 278% which is promising enough to withhold any kind of pavements. Other than pavements, this stabilized soil can also be applied in the construction of major highways. The CBR test results also indicate that the stabilizers are strong enough to be applied in the mega projects with the increment of the appropriate amount of dosage.

CHAPTER 5
Conclusion & Future Scopes

5.1 Conclusion

The sandy soil properties experienced a notable change due to the addition of the mixture of the stabilizers which results in the significant increase of the UCS values exceeding 200 kPA, alongside CBR values exceeding 80% particularly pronounced after a 28-day curing period. The SB-95 content played a leading role in achieving the soil strength with the help of adhering the soil with the stabilizers using TX-95 content. The effectiveness of the stabilizers enhances the load-bearing capacity of the soil with the increased dosage of SB-95 content. The findings of the TX-95 & SB-95 content indicates that these stabilizers have the potential to be effectively applied as a soil stabilizing agent, consideration for diverse engineering applications such as road construction, embankments, and foundations, as integral components of soil improvement strategies.

5.2 Future Scopes

The impact of the variety of TX-95 dosage can be explored in the future research, offering in-depth analysis into its optimum concentration for achieving the desired soil stabilization effects. The cost-benefit analysis ratio of these stabilizers might be a significant interest for the future researchers. The further investigation of these additives can provide broad insights due to various geological contexts. Alternate testing methodologies can provide more comprehensive evaluation of the effectiveness of these stabilizers.

References

Abid, M. S. (2016). Stabilization of Soil using Chemical Additives . *GRD Journal for Engineering* , 74.

Afrin, H. (2017). A Review on Different Types Soil Stabilization Techniques. *International Journal of Transportation Engineering and Technology*, 20.

Ali Akbar Firoozi1*, C. G. (2017). Fundamentals of Soil Stabilization. *International Journal of Geo-Engineering*, 01.

Al-Rawas, A. A., Hago, A., & Al-Sarmi, H. (2005, May). Effect of lime, cement and Sarooj (artificial pozzolan) on the swelling potential of an expansive soil from Oman. *Building and Environment, 40*(5), 681-687.

Al-Rawas, A., & Goosen, M. F. (2006). *Expansive soils: Recent advances in characterization and treatment.* Taylor & Francis.

Archibong, G. A. (2020). A REVIEW OF THE PRINCIPLES AND METHODS OF SOIL. *International Journal of Advanced Academic Research* , 90.

Archibong, G. A. (2020). A REVIEW OF THE PRINCIPLES AND METHODS OF SOIL STABILIZATION. *International Journal of Advanced Academic Research*, 90.

Arif Ali Baig Moghal, P. M.-S. (2017). Target Reliability Approach to Study the Effect of Fiber Reinforcement on UCS Behavior of Lime Treated Semi-Arid Soil. *Journal of Materials in Civil Engineering*, 10.

Arinze, E. E. (2014). Effect of Rock-Sized Aggregates on Soil Compaction Results. *IOSR Journal of Mechanical and Civil Engineering (IOSR-JMCE)*, 31.

Ary Bruand, C. H. (2006). Physical properties of tropical sandy soils: A large range of behaviours . *HAL Open Science*, 1.

ASTM Aggregate and Soil Terminology. (n.d.). Retrieved from pavement ineractive: https://pavementinteractive.org/reference-desk/materials/aggregate/astm-aggregate-and-soil-terminology/

Bell, F. (1996). Lime stabilization of clay minerals and soils. *Engineering Geology, 42*(4), 223-237.

Burland, J. B. (2014). The Stabilization of the Leaning Tower of Pisa. *Journal of Architectural Conservation*, 7.

Chang, I., Im, J., & Cho, G.-C. (2016, March). Introduction of Microbial Biopolymers in Soil Treatment for Future Environmentally-Friendly and Sustainable Geotechnical Engineering. *Sustainability, 8*(3).

Cheng, L., & Cord-Ruwisch, R. (2012, May). In situ soil cementation with ureolytic bacteria by surface percolation. *Ecological Engineering, 42*, 64-72.

Chibuzor2, A. F. (2022). Improving resilient modulus and cyclic crack restriction of preloaded expansive subgrade treated with nano-geopolymer binder. *Arabian Journal of Geosciences* , 10.

Consoli, N. C., Prietto, P. D., & Pasa, G. S. (2011, July). The effect of curing time on the strength of artificially cemented soil. *Ground Improvement, 5*(2), 35-44.

Cox's Bazar Marine Drive crumbling into sea. (2023, August 03). Retrieved from Dhaka Tribune : https://www.dhakatribune.com/bangladesh/321585/cox's-bazar-marine-drive-crumbling-into-sea

Das, B. M. (2006). *Principles of Geotechnical Engineering Seventh Edition.* Cengage Learning.

DeJong, J. T., Mortensen, B. M., Martinez, B. C., & Nelson, D. C. (2010, February). Bio-mediated soil improvement. *Ecological Engineering, 36*(2), 197-210.

Design Manual. (2013). STATEWIDE URBAN DESIGN AND SPECIFICATIONS.

Friction Angle of Soils + Typical Values. (n.d.). Retrieved from Civilengineeringbible: https://civilengineeringbible.com/subtopics.php?i=89

H., D., Gray, B., R., & Sotir. (1996). *Biotechnical and soil bioengineering slope stabilization: a practical guide for erosion control.*

Hadi Fatehi 1, 2. ,. (2021). Biopolymers as Green Binders for Soil Improvement in Geotechnical Applications: A Review. *geosciences*, 21.

HANS F. WINTERKORN, D. p. (1991). *SOIL STABILIZATION AND GROUTING.* Van Nostrand Reinhold.

Ingles, O., & Metcalf, B. (1972). *SOIL STABILIZATION PRINCIPLES AND PRACTICE.* London.

Jingyi Huang□, A. E. (2020). Soil and environmental issues in sandy soils. *Earth-Science Reviews*, 2.

Jingyi Huang□, A. E. (2020). Soil and environmental issues in sandy soils. *Earth-Science Reviews*, 1.

Jones, J. (2017, September 14). *California bearing ratio typical values*. Retrieved from CBR Testing UK: https://www.cbrtesting.com/california-bearing-ratio-typical-values/#:~:text=What%20are%20the%20typical%20CBR%20values%3F%20The%20harder,with%20a%20maximum%20particle%20size%20of%2020%20mm.

Joseph E. Bowles, R. S. (1996). *FOUNDATION ANALYSIS AND DESIGN Fifth Edition.* McGraw-Hill Companies.

Karol, R. H. (2003). *Chemical grouting and soil stabilization.* CRC Press.

Khemissa, M., & Mahamedi, A. (2014, June). Cement and lime mixture stabilization of an expansive overconsolidated clay. *Applied Clay Science, 95*, 104-110.

Latifi, N., A. M., Rashid, A. S., & Yii, J. L. (2016). Strength and Physico-chemical Characteristics of Fly Ash–Bottom Ash Mixture. *Journal of Rock Mechanics and Geotechnical Engineering, 8*(6), 909-916.

Makusa, G. P. (2012). *SOIL STABILIZATION METHODS AND MATERIALS.* Luleå: Department of Civil, Environmental and Natural resources engineering, Division of Mining and Geotechnical Engineering , Luleå University of Technology .

Mane, V. (2020, November 23). *California Bearing Ratio Test【CBR Test】of Soil*. Retrieved from civilengineeringnotes: https://civilengineeringnotes.com/cbr-test/

MD Sahadat Hossain, P. P., Islam, M. A., & Fahim, F. (2021). *Properties and Behavior of Soil – Online Lab Manual.* Mavs Open Press.

MD Sahadat Hossain, P. P., Islam, M. A., Badhon, F. F., & Imtiaz, a. T. (2021). *Properties and Behavior of Soil – Online Lab Manual.* Mavs Open Press.

Michael Z. Izzo 1 and Marta Mileti´ c 2, *. (2022). Desiccation Cracking Behavior of Sustainable and Environmentally Friendly Reinforced Cohesive Soils. *Polymers*, 2.

Morgan, R. P. (2009). *Soil erosion and conservation(3rd ed.).* Blackwell Publishing.

Osman, K. T. (2018). Sandy Soils. *Management of Soil Problems*, 38.

Rahman Izadi, M. M. (2022). An Overview of Methods and Materials for Sandy soil stabilization: Emerging Advances and Current Applications. *ECOPERSIA* , 336.

Sakina Tamassoki 1, 2. ,. (2022). Compressive and Shear Strengths of Coir Fibre Reinforced Activated Carbon Stabilised Lateritic Soil. *Sustainability*, 1.

Sengupta, U. (2023, August 14). *Flood damage to Dohazari-Cox's Bazar rail tracks is a lesson to learn, says project director*. Retrieved from bdnews24.com: https://bdnews24.com/bangladesh/7l99a8f59v

Sherwood, P. (1993). *SOIL STABILIZATION WITH CEMENT AND LIME.* HMSO.

Shooshpasha, I., & Shirvani, R. A. (2015). Effect of cement stabilization. *Geomechanics and Engineering, 8*, 17-31.

Siddiquee, T. (n.d.). *Specific Gravity of Sand Soil – Standard & Test Procedure*. Retrieved from Civiltoday: https://civiltoday.com/civil-engineering-materials/sand/359-specific-gravity-of-sand#:~:text=The%20considerable%20specific%20gravity%20is%20around%202.65%20for,to%203.0%20with%20an%20average%20of%20about%202.68.

Sivakugan, N. (2006). *Introduction To Geotechnical Engineering Siva Sivakugan.*

Soil permeability coefficient. (2013, October 7). Retrieved from geotech data: https://www.geotechdata.info/parameter/permeability

Tim E. Kowalski and Dale W. Starry, J. (2007). Modern Soil Stabilization Techniques. *Annual Conference of the Transportation Association of Canada Saskatoon, Saskachewan* (p. 3). Saskatoon: Wirtgen America, Inc.

Tingle, J. S., & Santoni, R. L. (2003, January). Stabilization of Clay Soils with Nontraditional Additives. *Transportation Research Record*, 72-84.